



**SYNTHESIS, STRUCTURE AND DYNAMIC STUDIES
ON BASE-STABILIZED SILYLENE COMPLEXES
[(η^5 -C₅Me₅)(PMe₃)₂RuSiX₂(NCMe)⁺]^{†‡}**

STEVEN K. GRUMBINE,[§] DANIEL A. STRAUS^{||} and T. DON TILLEY[¶]

Department of Chemistry, University of California, Berkeley, CA 94720-1460, U.S.A.

and

ARNOLD L. RHEINGOLD

Department of Chemistry, University of Delaware, Newark, DE 19716, U.S.A.

Abstract—The silyl complexes Cp*(PMe₃)₂RuSiX₂Z (Cp* = η^5 -C₅Me₅; **1**, SiX₂Z = Si[S(Tol-*p*)]₃; **2**, SiX₂Z = Si[O(Tol-*p*)]₃; **3**, SiX₂Z = SiMe₂[S(Tol-*p*)]), prepared by reaction of the appropriate hydrosilane with Cp*(PMe₃)₂RuCH₂SiMe₃, react with Me₃SiOTf (OTf = OSO₂CF₃) to afford the triflate(silyl) complexes Cp*(PMe₃)₂RuSiX₂OTf (**4**, X = S(Tol-*p*); **5**, X = O(Tol-*p*); **6**, X = Me) or Cp*(PMe₃)₂RuSi[S(Tol-*p*)](OTf)₂ (**7**). The X-ray crystal structures of the compounds **1**, **4**, and **7** are described and discussed. Compound **4** reacts with LiBEt₃H to produce Cp*(PMe₃)₂RuSiH[S(Tol-*p*)]₂ (**8**), with water to give Cp*(PMe₃)₂RuSi[S(Tol-*p*)](OTf)(OH) (**10**), and with HCl to afford Cp*(PMe₃)₂RuSiCl₂(OTf) (**11**). The triflate Cp*(PMe₃)₂RuSiH[S(Tol-*p*)](OTf) (**9**) results from reaction of **8** with Me₃SiOTf. The base-stabilized silylene complexes [Cp*(PMe₃)₂RuSiX₂(NCMe)]BPh₄ (**13**, X = S(Tol-*p*); **14**, X = O(Tol-*p*); **15**, X = Me) are prepared by displacement of triflate from **4–6**. The X-ray structures of **13** and **15** are described and compared to the previously reported structure of [Cp*(PMe₃)₂RuSiPh₂(NCMe)]BPh₄ (**12**). The structures are discussed in terms of the amount of incipient silylene character possessed by each. For **12–15**, bound acetonitrile exchanges with free acetonitrile in dichloromethane solution via a dissociative mechanism. The rates and activation parameters for these exchange reactions allow an ordering of stabilities for the corresponding base-free silylene complexes, since the reactions involve rate-limiting loss of acetonitrile from the complex. The kinetic data indicate that the stabilizing influences for silylene substituents in this system are ordered according to: S(Tol-*p*) > O(Tol-*p*) > Me > Ph. A different ordering is suggested by the X-ray structural data. Apparently conflicting information from the structural and dynamic studies are discussed and rationalized, and it is concluded that the ordering suggested by the kinetic data is more useful.

The development of transition-metal silylene chemistry reached a significant milestone in 1987, when two base-stabilized examples, [Cp*(PMe₃)₂RuSiPh₂(NCMe)]BPh₄ (Cp* = η^5 -C₅Me₅)¹ and

[†] Dedicated to Professor John E. Bercaw on the occasion of his 50th birthday.

[‡] Much of this work was carried out at the University of California at San Diego.

[§] Present address: Los Alamos National Laboratory, CST-3, Mail Stop C346, Los Alamos, NM 87545, U.S.A.

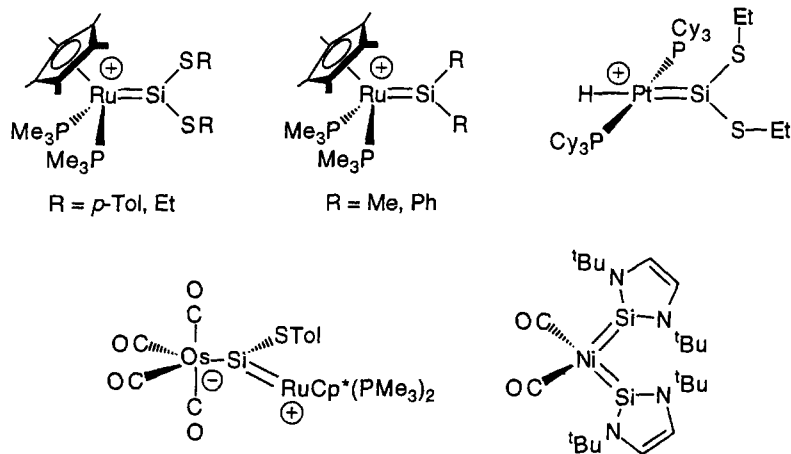
^{||} Present address: Chemistry Department, San Jose State University, San Jose, CA 95192-0101, U.S.A.

[¶] Author to whom correspondence should be addressed.

(CO)₄FeSi(O^tBu)₂(HMPA) (HMPA = hexamethylphosphoramide),² were independently discovered and structurally characterized.³ Over the past few years a number of related adducts have been synthesized, and currently there are nearly 20 crystallographically characterized examples in the literature.⁴ Many of these compounds are transition metal carbonyl derivatives synthesized by Zybll and coworkers.⁵ Additional examples of cationic ruthenium complexes of the type [Cp* (PMe₃)₂RuSiX₂(Base)]⁺ have also been reported.⁶ Ogino and coworkers have developed a route to unusual silylene derivatives, for example Cp* (CO) FeSiMe₂(μ-OMe)SiMe(OMe) and (CO)₄MnSiMe₂(μ-OMe)SiMe₂, in which two silylene fragments are bridged by a methoxide group.⁷ Other recently reported adducts of silylene complexes include Corriu's internally-stabilized L_nMSiH[C₆H₄(2-CH₂NMe₂)] (L_nM = (CO)₅Cr, (CO)₄Fe, Cp(CO)₂Mn),⁸ Jutzi and Möhrke's

clearly present in each case.^{4–10} As might be expected for compounds with some metal–silicon double bond character, the ²⁹Si NMR chemical shifts for base-stabilized complexes appear somewhat downfield from the shifts for analogous silyl derivatives. Thus, adducts of dialkylsilylene and diarylsilylene complexes give rise to ²⁹Si shifts in the range 70–130 ppm (an exception is (TTP)Os SiEt₂(THF), with a shift of only 25 ppm). Corresponding thiolate and chloride derivatives produce signals in the range 30–90 ppm, while L_nMSi(OR)₂(Base) derivatives give rise to ²⁹Si shifts much further upfield, at –5 to 15 ppm. These observed substituent effects on ²⁹Si chemical shifts (Me > SR > OR) parallel those seen in common silane derivatives.¹⁵

Recently, authentic silylene complexes possessing sp² silicon centers have finally been isolated and definitively characterized. The structures of all silylene complexes which have been reported to date are given below.



ClAuSi(η¹-Cp*)₂(Base) (Base = pyr, CN^tBu),⁹ Woo's (TTP)OsSiEt₂(THF) (TTP = tetra-*p*-tolylporphyrin),¹⁰ and the cationic [Cp(NO)(PPh₃)ReSiMe₂(pyr)]⁺ of Gladysz and coworkers.¹¹

A Lewis base stabilizes a silylene ligand by donating electron density to an otherwise electron-deficient silicon center, thus blocking a potentially reactive site. Similar stabilizing influences for a coordinated Lewis base have been documented for adducts of silamines (RN = SiR'₂ · Base),¹² silenes (R₂C = SiR'₂ · Base),¹³ and silylenium ions (R₃Si · Base⁺).¹⁴ A natural question that arises in investigations of base-stabilized silylene complexes concerns the degree to which true "silylene character" exists in these adducts. Solid-state structural data seems to provide some evidence for silylene character, though distorted tetrahedral silicon centers are

The first report, on [Cp*(PMe₃)₂Ru=Si(SR)₂]BPh₄ derivatives, appeared in 1990.¹⁶ Although these complexes have not been structurally characterized, they are readily identified by characteristic downfield ²⁹Si NMR resonances at 250–270 ppm. More recently, we have shown that it is possible to isolate the nonheteroatom-stabilized silylene complexes [Cp*(PMe₃)₂Ru=SiR₂]⁺ (R = Me, Ph) as B(C₆F₅)₄[–] salts.¹⁷ These compounds are less stable than the related thiolate derivatives but the crystal structure of [Cp*(PMe₃)₂Ru=SiMe₂]B(C₆F₅)₄, which contains a planar sp² silicon center (δ(²⁹Si) = 311), has been determined. The platinum complex [*trans*-(PCy₃)₂(H)Pt=Si(SET)₂]BPh₄ (δ(²⁹Si) = 309), like the previously described cationic silylene complexes, was obtained by exchange of a covalently-bound triflate anion for the non-

coordinating tetra(aryl)borate anion in dichloromethane.¹⁸ For this complex, molecular orbital calculations indicate that heteroatom $3_{p\pi}-3_{p\pi}$ donation plays a dominant role in stabilizing the three-coordinate silicon center. The zwitterionic, transition metal-substituted silylene complex $\text{Cp}^*(\text{PMe}_3)_2\text{Ru}=\text{Si}[\text{S}(\text{Tol-}p)][\text{Os}(\text{CO})_4]$, synthesized by displacement of two triflates in $\text{Cp}^*(\text{PMe}_3)_2\text{RuSi}[\text{S}(\text{Tol-}p)](\text{OTf})_2$ by $\text{Os}(\text{CO})_4^{2-}$, also contains an sp^2 silicon atom which appears to have a unique electronic environment based on its ^{29}Si NMR shift of δ 19.43.¹⁹ Finally, the recent preparation of a bis(silylene)nickel complex ($\delta(^{29}\text{Si}) = 97.5$) takes advantage of the remarkable isolation of the free silylene, which was used in a ligand substitution reaction with $\text{Ni}(\text{CO})_4$ to afford the complex shown above.²⁰

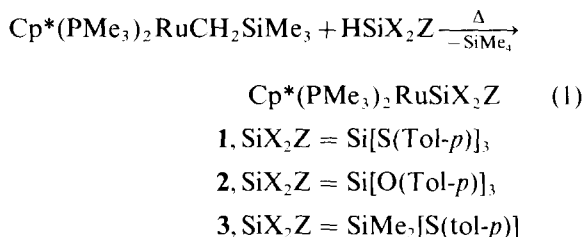
A general description of the electronic and chemical properties of silylene complexes is just emerging. It is clear that $\text{L}_n\text{M} = \text{SiX}_2$ compounds are inherently strong Lewis acids, and this characteristic will undoubtedly play a large role in defining their reactivity patterns. Studies on the base-complexed derivatives should therefore continue to provide useful information on the coordination chemistry of silylenes. Many base-stabilized silylene complexes, particularly those involving electron-poor $(\text{CO})_n\text{M}$ fragments, bind donors so tightly that dissociation is not observed even at elevated temperatures.^{5f,g} Exceptions to this rule include $(\text{CO})_4\text{MnSiMe}_2(\mu\text{-OMe})\text{SiMe}_2$, which rapidly exchanges its bridging methoxy group for CD_3O in CD_3OH ,^{7c} and $(\text{CO})_5\text{CrSi}[\text{C}_6\text{H}_4(2\text{-CH}_2\text{NMe}_2)]_2$, which undergoes degenerate, intramolecular, associative substitutions.^{5h} For base-stabilized silylene complexes of the $\text{Cp}^*(\text{PMe}_3)_2\text{Ru}^+$ fragment, the base is quite labile. For example, the bound acetonitrile in $[\text{Cp}^*(\text{PMe}_3)_2\text{RuSiPh}_2(\text{NCMe})]\text{BPh}_4$ exchanges rapidly with free acetonitrile in solution via a dissociative mechanism.^{6a} Here we describe the synthesis and study of a family of base-stabilized silylene complexes of the type $[\text{Cp}^*(\text{PMe}_3)_2\text{RuSiX}_2(\text{Base})]^+$. As detailed below, structural and dynamic studies on these compounds contribute to our understanding of electronic influences on the stability of silylene complexes.

RESULTS AND DISCUSSION

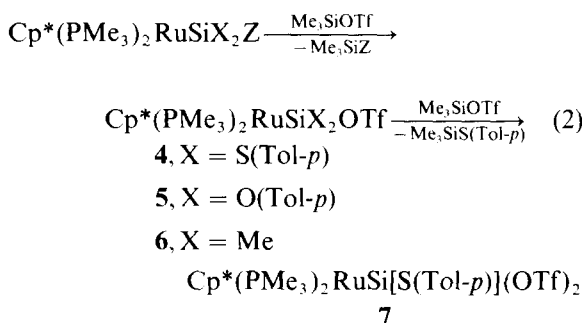
Synthesis of new ruthenium(II) silyl complexes

The starting ruthenium(II) silyl complexes were synthesized according to our previously described method, based on reaction of $\text{Cp}^*(\text{PMe}_3)_2\text{RuCH}_2\text{SiMe}_3$ with a hydrosilane at 90–105°C (eq.

(1)).^{6a} The light-yellow, air-sensitive complexes **1–3** were completely characterized spectroscopically and by elemental analyses.

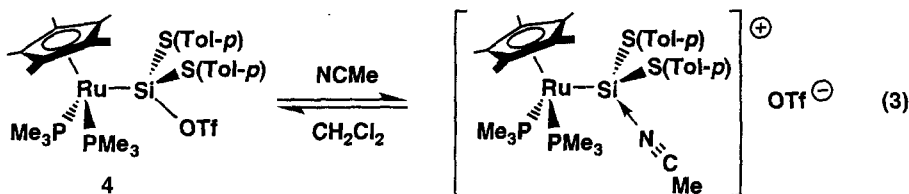


A triflate substituent is readily incorporated into the silyl ligands via treatment of **1–3** with Me_3SiOTf (eq. (2), $\text{OTf} = \text{OSO}_2\text{CF}_3$). The resulting triflate(silyl) complexes **4–6** are less soluble in hydrocarbons than their precursor complexes, making them relatively easy to crystallize. Extended reaction (4 days) of compound **1** with an excess (4 equivalents) of Me_3SiOTf in dichloromethane results in exchange of two thiolate groups to produce the bis(triflate) derivative **7** in 78% yield (eq. (2)).



We have previously shown that silyl complexes related to **4–7** possess chemically labile triflate groups. For example, the triflate in $\text{Cp}^*(\text{PMe}_3)_2\text{RuSiPh}_2\text{OTf}$ is displaced in acetonitrile solution to give a base-stabilized silylene complex.^{6a} The triflate group of $\text{Cp}^*(\text{PMe}_3)_2\text{RuSi}(\text{SET})_2\text{OTf}$ reversibly dissociates in dichloromethane to form the transient silylene complex $[\text{Cp}^*(\text{PMe}_3)_2\text{Ru}=\text{Si}(\text{SET})_2]^+\text{OTf}^-$, as determined by variable-temperature NMR experiments.¹⁶ The triflate groups of complexes **4–7** are also labile, but covalently bound in the solid state as indicated by infrared $\nu(\text{SO}_3)$ vibrational modes at *ca* 1360 cm^{-1} .²¹ Compound **4** displays an infrared absorption for covalently bound triflate (1362 cm^{-1}) in dichloromethane solution, but in acetonitrile only ionic triflate is detected (eq. (3), $\nu(\text{SO}_3) = 1269 \text{ cm}^{-1}$). Concordantly, conductivity measurements indicate a neutral structure in dichloromethane (8 $\Omega \text{ cm}^2 \text{ equiv}^{-1}$) and ionization in acetonitrile (133 $\Omega \text{ cm}^2 \text{ equiv}^{-1}$).

Interestingly, the bis(triflate) **7** exhibits solution



behavior that is very similar to that observed for **4**. Thus, an associated structure exists in dichloromethane ($\nu(\text{SO}_3) = 1377 \text{ cm}^{-1}$; conductivity = $3 \text{ } \Omega \text{ cm}^2 \text{ equiv}^{-1}$) while a dissociated one is observed in acetonitrile ($\nu(\text{SO}_3) = 1271 \text{ cm}^{-1}$; conductivity = $131 \text{ } \Omega \text{ cm}^2 \text{ equiv}^{-1}$). The similarity in conductivity values for **4** and **7** suggests that **7** may exist in solution as the "silylene" $\{\text{Cp}^*(\text{PMe}_3)_2\text{RuSi}[\text{S}(\text{Tol-}p)](\text{OTf})(\text{NCMe})\}^+(\text{OTf})^-$, however this is not supported by the infrared data. The infrared spectrum of **7** in acetonitrile contained only the vibrational mode for ionic triflate, and covalently bound triflate was not detected. Therefore in acetonitrile, **7** probably exists primarily as the base-complexed silylyne derivative $\{\text{Cp}^*(\text{PMe}_3)_2\text{RuSi}[\text{S}(\text{Tol-}p)](\text{NCMe})_2\}^{2+}(\text{OTf}^-)_2$, analogous to the previously reported complexes $\{\text{Cp}^*(\text{PMe}_3)_2\text{RuSi}[\text{S}(\text{Tol-}p)](\text{L}_2)\}^{2+}$ ($\text{L}_2 = \text{bipy}, \text{phen}$).^{6b} Thus, the conductivity value for **7** appears to reflect extensive ion-pairing for $\{\text{Cp}^*(\text{PMe}_3)_2\text{RuSi}[\text{S}(\text{Tol-}p)](\text{NCMe})_2\}^{2+}(\text{OTf}^-)_2$ in acetonitrile.²² Unfortunately, attempts to isolate $\{\text{Cp}^*(\text{PMe}_3)_2\text{RuSi}[\text{S}(\text{Tol-}p)](\text{NCMe})_2\}^{2+}(\text{OTf}^-)_2$ were thwarted by its relatively rapid ($t_{1/2} \approx 2 \text{ h}$) decomposition in acetonitrile solution, to numerous products.

Previously, ²⁹Si NMR shifts for transition-metal silicon compounds have been correlated with metal–silicon double bond character. Whereas such a correlation appears to hold for $\text{Cp}^*(\text{PMe}_3)_2\text{RuSiPh}_2\text{OTf}$,^{6a} the trend in ²⁹Si NMR shifts for **1** ($\delta 49.03$; $J_{\text{SiP}} = 34 \text{ Hz}$), **4** ($\delta 77.14$; $J_{\text{SiP}} = 36 \text{ Hz}$), and **7** ($\delta 37.10$; $J_{\text{SiP}} = 39 \text{ Hz}$) is not readily interpretable in terms of increasing "silylene character".

Reactions of the triflate(silyl) complex $\text{Cp}^*(\text{PMe}_3)_2\text{RuSi}[\text{S}(\text{Tol-}p)]_2(\text{OTf})$ (**4**)

The triflate derivatives described above have proven to be versatile starting materials for the synthesis of new ruthenium–silicon bonded complexes. For example, compound **7** has been used to prepare the base-stabilized silylyne complexes $\{\text{Cp}^*(\text{PMe}_3)_2\text{RuSi}[\text{S}(\text{Tol-}p)](\text{L}_2)\}^{2+}$ ($\text{L}_2 = \text{bipy}, \text{phen}$)^{6a} and the transition metal-substituted silylene complexes $\text{Cp}^*(\text{PMe}_3)_2\text{RuSi}[\text{S}(\text{Tol-}p)]\text{M}(\text{CO})_4$

($\text{M} = \text{Fe}, \text{Os}$).^{19,23} We report here a brief examination of the reactivity of the mono(triflate) **4** (Scheme 1).

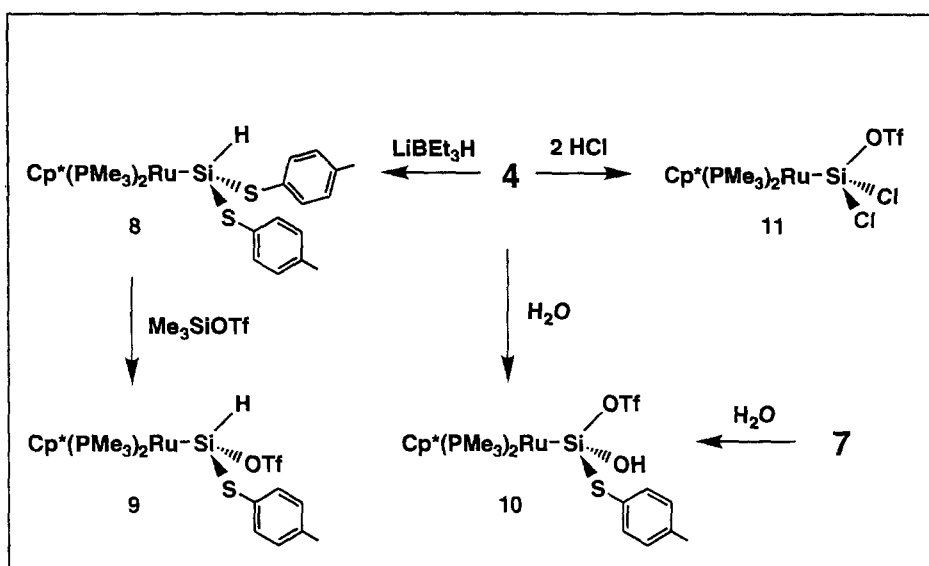
Reaction of **4** with the nucleophilic reagent $\text{LiB Et}_3\text{H}$ displaces triflate to yield the hydrosilyl complex **8**. Compound **8** exhibits a $\nu(\text{SiH})$ infrared stretching frequency at 2058 cm^{-1} , and the ²⁹Si NMR resonance for **8** ($\delta 67.95$) is a doublet of triplets resulting from coupling of the silicon to both hydrogen ($^1J_{\text{SiH}} = 191 \text{ Hz}$) and phosphorus ($^2J_{\text{SiP}} = 31 \text{ Hz}$). Exchange of a thiolate substituent in **8** for a triflate group occurs readily upon reaction with Me_3SiOTf , to afford **9**. As expected, the ²⁹Si NMR shift for **9** ($\delta 88.81$, $^1J_{\text{SiH}} = 196 \text{ Hz}$, $^2J_{\text{SiP}} = 31 \text{ Hz}$) is downfield-shifted relative to that for **8**, but only by *ca* 20 ppm. The ³¹P{¹H} NMR spectrum of **9** at room temperature in dichloromethane-*d*₂, which contains resonances for inequivalent phosphorus nuclei at $\delta 2.16$ and 3.54 ($^2J_{\text{PP}} = 38 \text{ Hz}$), is consistent with a stereochemically rigid structure with a chiral silicon center.

Hydrolysis of **4** gives an isolable silanol derivative (**10**), which may also be obtained by addition of water to **7**. The silanol proton of **10** ($\delta 4.78$) exhibits equivalent coupling to both phosphorus nuclei ($^4J_{\text{HP}} = 7 \text{ Hz}$), and at 23°C a single peak is observed in the ³¹P{¹H} NMR spectrum at $\delta -0.60$ (dichloromethane-*d*₂). The latter observation strongly suggests that racemization at silicon occurs rapidly in solution via the intermediate silylene complex $\{\text{Cp}^*(\text{PMe}_3)_2\text{Ru}=\text{Si}[\text{S}(\text{Tol-}p)]\text{OH}\}^+\text{OTf}^-$.¹⁶ The observed $\nu(\text{OH})$ stretching frequency for **10** (2438 cm^{-1}) is unusually low, indicating the presence of hydrogen bonding to the triflate group. For comparison, complexes of the type $\text{Cp}(\text{PPh}_3)(\text{CO})\text{FeSiR}_2\text{OH}$ display "normal" $\nu(\text{OH})$ stretching frequencies in the range $3600\text{--}3700 \text{ cm}^{-1}$.²⁴

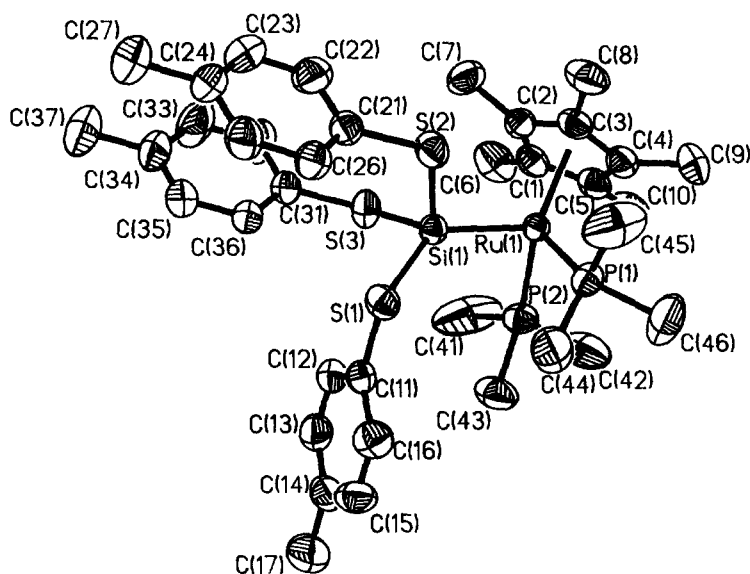
The reaction of **4** with HCl also leads to clean removal of thiolate groups, in this case to produce **11**, isolated as light yellow crystals from toluene in 75% yield.

X-ray structures of the triflates **1**, **4**, and **7**

The molecular structures of **1**, **4**, and **7** are shown in Figs 1–3, crystallographic data in Table 1 and



Scheme 1.

Fig. 1. ORTEP view of the molecular structure of $\text{Cp}^*(\text{PMe}_3)_2\text{RuSi}[\text{S}(\text{Tol-}p)]_3$ (**1**).

important geometrical parameters for these complexes are listed in Tables 2–4. The three structures are similar in that each possesses a “three-legged piano stool” coordination geometry for the ruthenium, and distorted tetrahedral coordination for silicon. Compound **4**, like $\text{Cp}^*(\text{PMe}_3)_2\text{RuSiPh}_2\text{OTf}$,^{6a} has a staggered conformation about the Ru—Si bond, with the Cp* and OTf groups in an anti relationship (Cp* centroid—Ru—Si—O dihedral angle = 176.3°). Overall, the observed bond distances and angles imply that the S(Tol-*p*) groups are more sterically demanding than the

triflates. This is undoubtedly a consequence of the relatively acute Si—S—C angles (*ca* 110–115°; *cf* 136–138° for the Si—O—S angles), and is reflected in somewhat longer Si—S bonds, and a wider variation in Ru—Si—S bond angles (132.5(1), 106.3(1), and 107.8(1)°) for **1**.

Steric factors may therefore play a role in the contraction of Ru—Si bond distances from **1** (2.350(1) Å) to **4** (2.306(2) Å) to **7** (2.269(3) Å), however the magnitudes of these differences (≈ 0.04 Å) suggest that electronic factors may also be important. We have previously suggested, based on

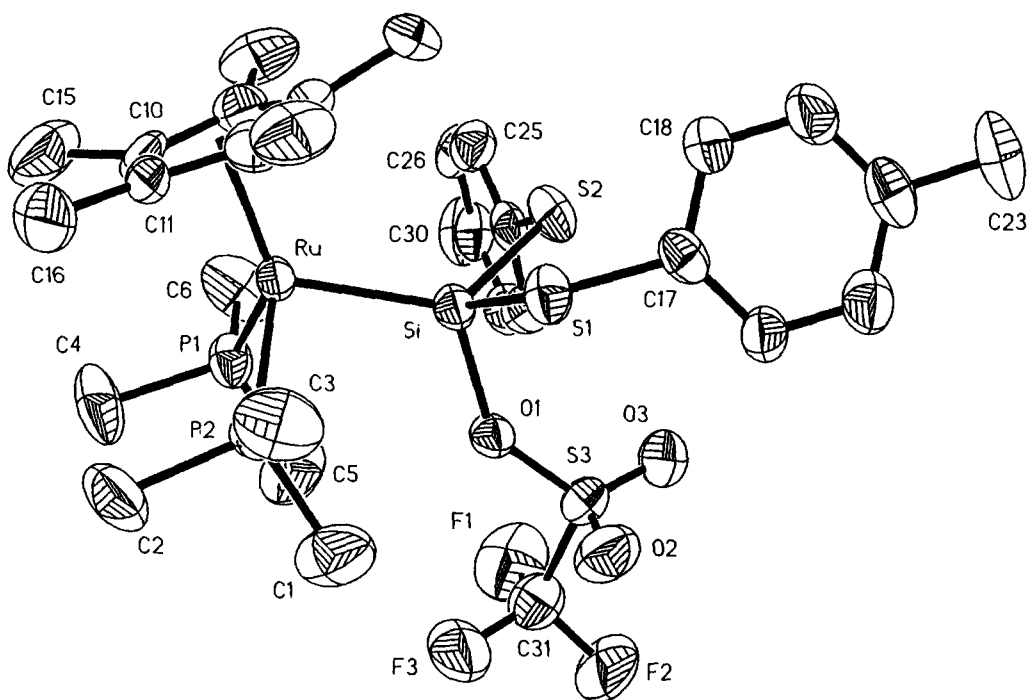


Fig. 2. ORTEP view of the molecular structure of $\text{Cp}^*(\text{PMe}_3)_2\text{RuSi}[\text{S}(\text{Tol-}p)]_2\text{OTf}$ (**4**).

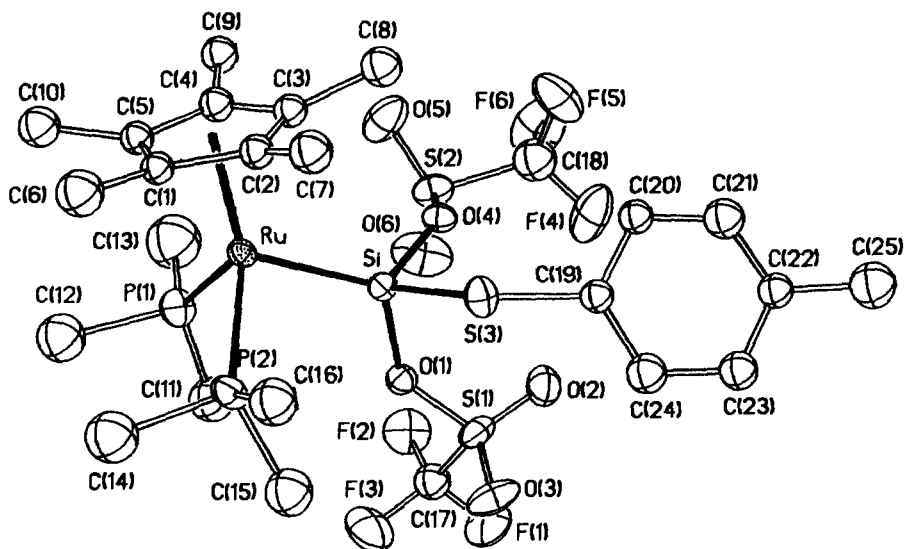


Fig. 3. ORTEP view of the molecular structure of $\text{Cp}^*(\text{PMe}_3)_2\text{RuSi}[\text{S}(\text{Tol-}p)](\text{OTf})_2$ (**7**).

structural and NMR data, that $\text{Cp}^*(\text{PMe}_3)_2\text{RuSiPh}_2\text{OTf}$ has significant "silylene character".^{6a} Similarly, silylene character for **4** is suggested by the relatively long Si—O bond distance of 1.856(5) Å. Typical Si—O bond lengths are in the range 1.63–1.66 Å,²⁵ and the analogous Si—O distance in $\text{Cp}^*(\text{PMe}_3)_2\text{RuSiPh}_2\text{OTf}$ is 1.853(5) Å. The

Si—O(triflate) distances are significantly longer than the Si—O distances in base-stabilized silylene complexes of the type $(\text{CO})_n\text{MSiX}_2(\text{HMPA})$ ($n = 5$, $\text{M} = \text{Cr}$; $n = 4$, $\text{M} = \text{Fe}$), which vary from 1.68 to 1.78 Å,^{4c,5} and slightly longer than the Si—O distance in $(\text{TTP})\text{OsSiEt}_2(\text{THF})$, 1.82 Å.¹⁰

Complexes of the type $\text{Cp}^*(\text{PMe}_3)_2\text{RuSiX}_2\text{OTf}$

Table 1. Crystallographic data for compounds **1**, **4**, and **7**

Chemical formula	C ₃₇ H ₅₄ P ₂ RuS ₃ Si (1)	C ₃₁ H ₄₇ F ₃ O ₃ P ₂ RuS ₃ Si (4)	C ₂₅ H ₄₀ F ₆ O ₆ P ₂ RuS ₃ Si (7)
<i>a</i> (Å)	11.293(3)	10.634(4)	11.0350(23)
<i>b</i> (Å)	13.354(4)	9.886(4)	17.3180(20)
<i>c</i> (Å)	14.681(4)	35.306(16)	18.7534(33)
α (°)	103.40(2)		
β (°)	91.16(2)	97.79(3)	
γ (°)	111.30(2)		
<i>V</i> (Å ³)	1993.2(10)	3678(3)	3583.9(11)
<i>Z</i>	2	4	4
Formula weight	786.1	812.0	837.7
Space group	<i>P</i> $\bar{1}$	<i>P</i> 2 ₁ / <i>c</i>	<i>P</i> 2 ₁ 2 ₁
<i>T</i> (°C)	23	23	24
λ (Å)	0.71073	0.71073	0.71073
ρ_{calc} (g cm ⁻³)	1.310	1.467	1.552
μ (Mo- <i>K</i> _α) (cm ⁻¹)	6.68	7.43	7.82
<i>R</i>	0.0339	0.0491	0.0448
<i>R</i> _w	0.0461	0.0568	0.0467

Table 2. Selected bond distances (Å) and angles (°) for Cp*(PMe₃)₂RuSi[S(Tol-*p*)]₃ (**1**)

Bond distances			
Ru(1)—Si(1)	2.350(1)	Si(1)—S(3)	2.196(1)
Ru(1)—P(1)	2.298(1)	S(1)—C(11)	1.773(4)
Ru(1)—P(2)	2.299(1)	S(2)—C(21)	1.788(5)
Si(1)—S(1)	2.223(1)	S(3)—C(31)	1.787(5)
Si(1)—S(2)	2.195(1)		
Bond angles			
P(1)—Ru(1)—P(2)	93.2(1)	Si(1)—S(1)—C(11)	113.9(1)
P(1)—Ru(1)—Si(1)	91.7(1)	Si(1)—S(2)—C(21)	112.8(1)
P(2)—Ru(1)—Si(1)	94.1(1)	Si(1)—S(3)—C(31)	116.8(1)
Ru(1)—Si(1)—S(1)	132.5(1)	S(1)—Si(1)—S(2)	91.1(1)
Ru(1)—Si(1)—S(2)	106.3(1)	S(1)—Si(1)—S(3)	106.0(1)
Ru(1)—Si(1)—S(3)	107.8(1)	S(2)—Si(1)—S(3)	111.5(1)

would therefore appear to have some silylene character, as evidenced by their solid state structures and by their lability in solution. However, another explanation for the short Ru—Si bonds which accompany long Si—O(triflate) distances in these systems can be based on $d_{\pi}-\sigma^*$ π -bonding involving donation of d -electron density from the metal center to a σ^* orbital based on the silyl ligand.^{4a,b,26} Such $d_{\pi}-\sigma^*$ donation should be heavily favored by the high electronegativity of the triflate group, which contributes to greater $d_{\pi}-\sigma^*$ overlap by concentrating much of the σ^* orbital in the vicinity of the metal atom. The shorter Si—O(triflate) distances in **7**, 1.780(7) and 1.765(8) Å, are perhaps a consequence of the competition of two σ^* orbitals for electron density from ruthenium, which results in less antibonding character per Si—O bond.

Synthesis and characterization of base-stabilized silylene complexes [Cp*(PMe₃)₂RuSiX₂(NCMe)]⁺

As described above, triflate anions dissociate from triflate(silyl) ruthenium complexes in acetonitrile solution to give cationic, base-stabilized silylene complexes. Following the methodology developed for the synthesis of [Cp*(PMe₃)₂RuSiPh₂(NCMe)]BPh₄ (**12**),^{1,6a} new acetonitrile-complexed silylenes **13–15** can be isolated after exchange of the triflate anion for BPh₄⁻. In general, these complexes are prepared by addition of 10–50 equivalents of NCMe to a dichloromethane solution of the triflate, and precipitation of NaOTf by reaction with NaBPh₄ (eq. (4)). Crystallization of the light yellow products from diethyl ether/dichloromethane provides moderate yields (35–

Table 3. Selected bond distances (Å) and angles (°) for Cp*(PMe₃)₂RuSi[S(Tol-*p*)]₂OTf (4)

Bond distances			
Ru—Si	2.306(2)	Si—O(1)	1.855(5)
Ru—P(1)	2.297(2)	S(1)—C(17)	1.788(5)
Ru—P(2)	2.304(3)	S(2)—C(24)	1.787(5)
Si—S(1)	2.188(3)	S(3)—O(1)	1.502(5)
Si—S(2)	2.180(3)		
Bond angles			
P(1)—Ru—P(2)	93.3(1)	Si—S(1)—C(17)	111.6(2)
P(1)—Ru—Si	95.0(1)	Si—S(2)—C(24)	109.0(2)
P(2)—Ru—Si	92.4(1)	Si—O(1)—S(3)	136.8(3)
Ru—Si—S(1)	110.2(1)	O(1)—S(3)—O(2)	112.8(3)
Ru—Si—S(2)	126.3(1)	O(1)—S(3)—O(3)	113.2(4)
Ru—Si—O(1)	117.3(2)	O(2)—S(3)—O(3)	119.3(4)
S(1)—Si—S(2)	97.8(1)	O(1)—S(3)—C(31)	99.2(4)
S(1)—Si—O(1)	102.9(2)	O(2)—S(3)—C(31)	104.4(5)
S(2)—Si—O(1)	98.6(2)	O(3)—S(3)—C(31)	105.0(4)

Table 4. Selected bond distances (Å) and angles (°) for Cp*(PMe₃)₂RuSi[S(Tol-*p*)](OTf)₂ (7)

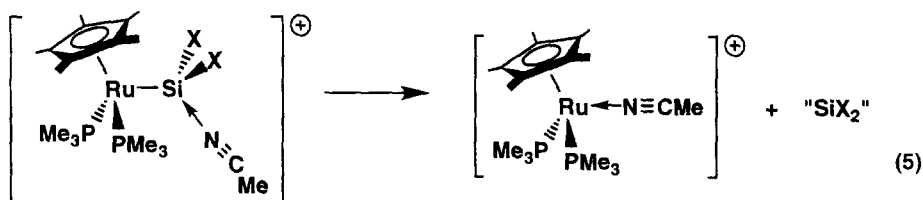
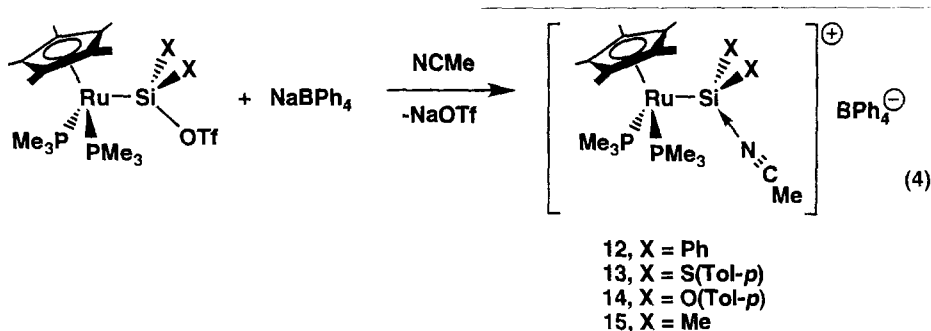
Bond distances			
Ru—Si	2.269(3)	Si—O(4)	1.765(8)
Ru—P(1)	2.297(3)	S(3)—C(19)	1.789(10)
Ru—P(2)	2.318(3)	S(1)—O(1)	1.524(6)
Si—S(3)	2.159(4)	S(2)—O(4)	1.520(8)
Si—O(1)	1.780(7)		
Bond angles			
P(1)—Ru(1)—P(2)	93.1(1)	S(3)—Si—O(1)	104.7(3)
P(1)—Ru—Si	95.2(1)	S(3)—Si—O(4)	98.8(3)
P(2)—Ru—Si	91.0(1)	O(1)—Si—O(4)	94.9(4)
Ru—Si—S(3)	111.4(2)	Si—S(3)—C(19)	116.3(4)
Ru—Si—O(1)	121.4(2)	Si—O(1)—S(1)	135.9(4)
Ru—Si—O(4)	121.9(3)	Si—O(4)—S(2)	138.1(4)

70%) of the products. With the stronger donor 4-dimethylaminopyridine (DMAP), this procedure allows isolation of [Cp*(PMe₃)₂RuSiMe₂(DMAP)]BPh₄ (**16**) in 29% yield. Unfortunately, attempts to use the reaction conditions of eq. (4) to obtain silylene complexes from triflates **9–11** led only to complex mixtures, which always included [Cp*(PMe₃)₂Ru(NCMe)]BPh₄ as a major product.

In the solid state, compounds **12–15** are stable for long periods, but they decompose slowly in solution. The room temperature decomposition of the dimethylsilylene complex **15** in dichloromethane-*d*₂ (*t*_{1/2} = 17 days) proceeds to [Cp*(PMe₃)₂Ru(NCMe)]BPh₄ (90%) and [Cp*(PMe₃)₂Ru(H)(Cl)]BPh₄ (4%). Under similar conditions the

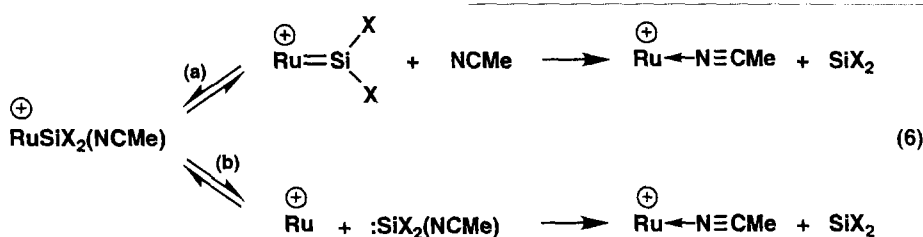
diphenylsilylene complex **12** decomposes more slowly, such that after 9 days only 10% of the decomposition product [Cp*(PMe₃)₂Ru(NCMe)]BPh₄ has formed. Complex **13** is even more stable than **12** (no decomposition is observed in solution over 2 weeks), and the overall ordering of solution decomposition rates for the acetonitrile adducts is **15** > **12** > **14** > **13**.

Thermal decompositions of **12–15** lead predominantly to displacement of the silylene ligand by acetonitrile (eq. (5)), and related processes are commonly observed in reactions of these adducts with various Lewis donors.²³ It is currently unclear how these silylene elimination reactions occur. Conceivably, the silylene fragment is lost dissociatively as the free silylene in two distinct steps (path (a), eq.



(6)), or perhaps as the silylene adduct $:\text{SiX}_2(\text{NCMe})$ (path (b)). Mechanistic and kinetic experiments have so far been severely complicated by the formation of varying amounts of minor side products. In the presence of the silylene traps HSiEt_3 , $\text{Me}_3\text{SiC}\equiv\text{CH}$, $\text{PhC}\equiv\text{CPh}$, and $\text{Si}(\text{OEt})_4$, free silylene species were not intercepted in the decompositions of **13** or **15**.

decomposition of *ca* 28 days. In this case, $[\text{Cp}^*(\text{PMe}_3)_2\text{Ru}(\text{NCMe})]\text{BPh}_4$ is still the major decomposition product. Assuming that the rate-limiting step in these reactions is loss of a silylene ligand (path (a) or (b) above), then it would appear that compound **15** may decompose via initial loss of acetonitrile to form the base-free silylene complex $[\text{Cp}^*(\text{PMe}_3)_2\text{Ru}=\text{SiMe}_2]\text{BPh}_4$. Consistent with



The effect of excess acetonitrile on these silylene elimination reactions is dramatic. Addition of 60 equivalents of acetonitrile to a dichloromethane- d_2 solution of **13** accelerates the rate of decomposition, to $t_{1/2} \approx 5$ h. However, these reaction conditions change the course of the decomposition, such that $[\text{Cp}^*(\text{PMe}_3)_2\text{Ru}(\text{NCMe})]\text{BPh}_4$ is no longer the major product, but is formed in only 5% yield along with seven other compounds (by ^{31}P NMR spectroscopy). The dimethylsilylene complex **15**, however, is stabilized in the presence of 60 equivalents of acetonitrile, resulting in a half-life for

this, the DMAP adduct **16** is more stable than **15** (3% decomposition after 1 day in dichloromethane- d_2), indicating that stronger donors give more stable complexes.

The ^{29}Si NMR chemical shifts for related silyl and silylene complexes are compared in Table 5. First note that for $\text{Cp}^*(\text{PMe}_3)_2\text{Ru}$ -silyl complexes, simple changes in the substituents at silicon can have a dramatic influence on the magnitude of the shift, such that variations over at least 75 ppm are observed. The relatively large downfield shift that is observed upon formation of the triflate probably

Table 5. ^{29}Si NMR data for selected $[\text{Cp}^*(\text{PMe}_3)_2\text{RuSiX}_2\text{Z}]^{0/+}$ silyl and silylene complexes^a

X	Z = X	Z = OTf	Z = NCMe	$[\text{Cp}^*(\text{PMe}_3)_2\text{Ru}=\text{SiX}_2]^+$
S(Tol- <i>p</i>)	49.0(34)	77.1(36)	58.3(39)	259.4(34) ^b
O(Tol- <i>p</i>)	-1.2(42)	0.0(45)	14.3(47)	
Me	20.0(28) ^c	133.3(33)	110.0(30)	311.4 ^d
Ph	74.1(30) ^e	112.4(33)	95.8 ^f	299(32) ^f

^aChemical shifts are in ppm, relative to SiMe_4 . $^2J_{\text{SiP}}$ coupling constants (Hz) are given in parentheses.

^bRef. 16.

^cRef. 23.

^dBroad singlet; coupling not resolved. Ref. 17.

^eX = Cl; ref. 6a.

^fRef. 17.

Table 6. Crystallographic data for compounds **13** and **15**

Chemical formula	$\text{C}_{56}\text{H}_{70}\text{BNP}_2\text{RuS}_2\text{Si}$ (13)	$\text{C}_{44}\text{H}_{62}\text{BNP}_2\text{RuSi}$ (15)
<i>a</i> (Å)	34.056(6)	16.997(5)
<i>b</i> (Å)	16.7163(23)	10.149(3)
<i>c</i> (Å)	9.4134(16)	25.661(7)
β (°)		101.00(2)
<i>V</i> (Å ³)	5359.0(16)	4345(2)
<i>Z</i>	4	4
Formula weight	1023.09	806.9
Space group	<i>Pn</i> 2 ₁ <i>a</i>	<i>P</i> 2 ₁ / <i>c</i>
<i>T</i> (°C)	23	-43
λ (Å)	0.71073	0.71073
ρ_{calc} (g cm ⁻³)	1.268	1.233
μ (Mo- <i>K</i> α) (cm ⁻¹)	4.77	4.92
<i>R</i>	0.0590	0.0696
<i>R</i> _w	0.0579	0.0805

reflects greater multiple bond character in the Ru—Si bond, which may be described in terms of “silylene character” and/or $d_{\pi}-\sigma^*$ backbonding. Formation of the acetonitrile adducts from the corresponding triflate is generally accompanied by an upfield shift of *ca* 15–25 ppm. This is consistent with the fact that acetonitrile is a stronger donor than triflate anion, and suggests that perhaps the triflate complexes possess greater “silylene character”. However, the differences in chemical shift between corresponding triflate and acetonitrile derivatives pale in significance when compared to the shifts for authentic silylene complexes (Table 5), and this emphasizes the true nature of the triflate and acetonitrile adducts as tetravalent silicon species, more related to silyl (sp^3 silicon) complexes than to silylene (sp^2 silicon) complexes.

Comparison of the structures of base-stabilized silylene complexes **12**, **13**, and **15**

The structure of **12** has been described previously.^{6a} Views of the cations in **13** and **15** are

given in Figs 4 and 5, and selected bond distances and angles are listed in Tables 7 and 8, respectively. For **15** the three legs of the piano stool structure are rotationally disordered about the Cp* centroid-Ru axis between two sites in a 78:22 ratio. The methyl groups are shared between sites and were refined at unit occupancy, and the minority-site molecule of CH₃CN was not located. Because of this disorder, the geometric parameters for **15** should be given less weight in the following discussion.

The staggered conformations about the Ru—Si bonds of **13** and **15** are similar to those observed for Cp*(PMe₃)₂RuSiPh₂X (X = H, OTf)^{6a} and **4**, in that the acetonitrile group is in a position anti to the Cp* ligand (Cp* centroid-Ru—Si—N dihedral angles are 170.4° for **13** and 169.4° for **15**). This contrasts with the situation for **12**, which has one nearly eclipsed P—Ru—Si—C(phenyl) dihedral angle (15.1°), and a small Cp* centroid-Ru—Si—N dihedral angle of 38.0°. Since the barrier to rotation about the Ru—Si bond in adducts **12**, **13**, and **15**

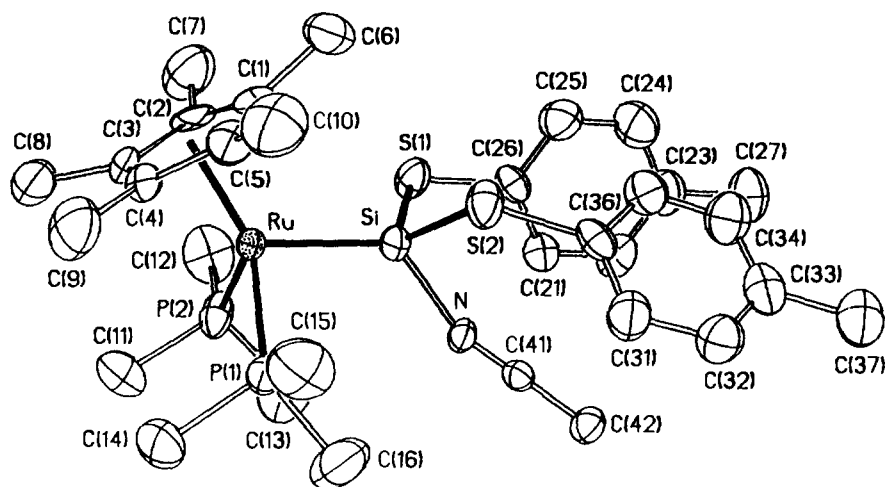


Fig. 4. ORTEP view of the molecular structure of $[\text{Cp}^*(\text{PMe}_3)_2\text{RuSi}[\text{S}(\text{Tol-}p)]_2(\text{NCMe})]\text{BPh}_4$ (**13**).

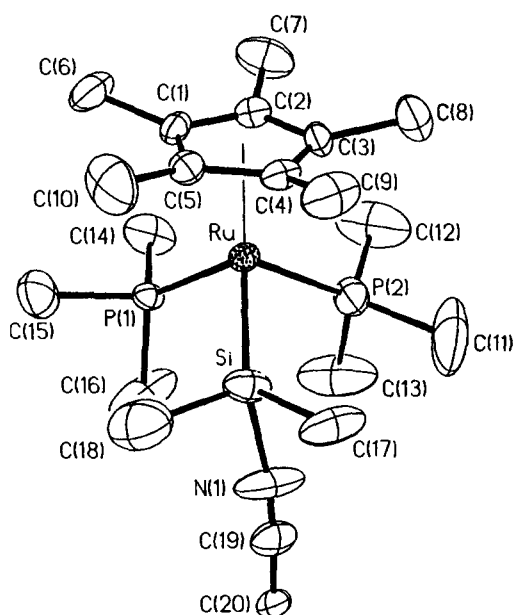


Fig. 5. ORTEP view of the molecular structure of $[\text{Cp}^*(\text{PMe}_3)_2\text{RuSiMe}_2(\text{NCMe})]\text{BPh}_4$ (**15**).

is expected to be very small, it seems that these conformations must be dictated primarily by steric and/or crystal packing effects. We have recently reported molecular orbital calculations which indicate that the preferred geometry for $[\text{Cp}(\text{PH}_3)_2\text{Ru}=\text{SiH}_2]^+$, which maximizes $\text{Ru}=\text{Si}$ double bonding, is such that the SiH_2 plane coincides with the mirror plane of the $\text{Cp}(\text{PH}_3)_2\text{Ru}^+$ fragment (dihedral angle = 0°).¹⁷ However, the observed dihedral angles of 68 and 34° , respectively, for the silylene complexes $\text{Cp}^*(\text{PMe}_3)_2\text{Ru}=\text{Si}[\text{S}(\text{Tol-}p)]$ $[\text{Os}(\text{CO})_4]$ ¹⁹ and $[\text{Cp}^*(\text{PMe}_3)_2\text{Ru}=\text{SiMe}_2]\text{B}(\text{C}_6\text{F}_5)_4$ ¹⁷ indicate that the electronic barrier to rotation about $\text{Cp}^*(\text{PMe}_3)_2\text{Ru}-\text{Si}$ bonds, even

when a full $\text{Ru}=\text{Si}$ double bond exists, is quite small.

In principle, it should be possible to evaluate the degree of metal-silicon multiple bonding in a base-stabilized silylene complex by analysis of the molecular structure. Thus, the magnitude of metal-silicon "bond shortening", or the degree of "planarization" at silicon might be expected to provide a measure of incipient silylene character. In the past, such analyses have suggested that some double bond character may exist in base-stabilized silylene complexes.⁴ Especially before structural data for authentic silylene complexes was available, it was tempting to use these "surrogate" base-stabilized structures to determine which substituents at silicon might stabilize a silylene ligand the most, according to which substituents lead to the most silylene-like structures.^{5d,f,g,6a} Such analyses are of course greatly complicated, and perhaps invalidated, by the fact that the silicon centers in base-stabilized silylene complexes are tetrahedral, and not very trigonal (or silylene-like), to begin with. Furthermore, multiple-bonding in late metal-silicon bonds is extremely difficult to quantify since multiple bonding appears to exist, to varying degrees, even in the silyl complexes.^{4a,b,26} Thus, it has proven difficult to establish reliable metal-silicon single bond lengths for d^n configurations above d^9 .

Table 9 lists various structural parameters which might be used to gauge the amount of incipient silylene character in the structures of **12**, **13**, and **15**. For comparison, the structures of corresponding silyl, triflate(silyl), and silylene complexes are also given. Firstly, the ruthenium-silicon bond length should reflect, to some degree, silylene character in the complex. Indeed, the $\text{Ru}-\text{Si}$ bond length of 2.28 Å for **13** is somewhat shorter than

Table 7. Selected bond distances (Å) and angles (°) for {Cp*(PMe₃)₂RuSi[S(Tol-*p*)]₂(NCMe)}BPh₄ (**13**)

Bond distances			
Ru—Si	2.284(3)	Si—N	1.866(9)
Ru—P(1)	2.292(3)	N—C(41)	1.147(13)
Ru—P(2)	2.284(4)	C(41)—C(42)	1.454(15)
Si—S(1)	2.181(5)	S(1)—C(26)	1.796(11)
Si—S(2)	2.177(5)	S(2)—C(36)	1.804(11)
Bond angles			
P(1)—Ru—P(2)	92.1(1)	S(1)—Si—N	95.6(3)
P(1)—Ru—Si	91.9(1)	S(2)—Si—N	92.5(3)
P(2)—Ru—Si	93.1(1)	S(1)—Si—S(2)	114.9(2)
Ru—Si—S(1)	111.8(2)	Si—N—C(41)	162.5(8)
Ru—Si—S(2)	112.7(2)	Si—S(1)—C(26)	112.2(4)
Ru—Si—N	127.7(2)	Si—S(2)—C(36)	111.5(4)

Table 8. Selected bond distances (Å) and angles (°) for [Cp*(PMe₃)₂RuSiMe₂(NCMe)]BPh₄ (**15**)^a

Bond distances			
Ru—Si	2.258(4), 2.190(14)	Si—C(18)	1.822(18)
Ru—P(1)	2.265(4), 2.293(16)	Si—N(1)	1.963(15)
Ru—P(2)	2.338(5), 2.378(16)	N(1)—C(19)	1.133(20)
Si—C(17)	1.838(14)	C(19)—C(20)	1.430(19)
Bond angles			
P(1)—Ru—P(2)	92.9(2), 91.3(5)	Ru—Si—N(1)	115.9(4)
P(1)—Ru—Si	94.9(2), 93.9(5)	C(17)—Si—N(1)	92.6(6)
P(2)—Ru—Si	92.0(2), 94.3(6)	C(18)—Si—N(1)	98.7(8)
Ru—Si—C(17)	125.5(5)	C(17)—Si—C(18)	102.8(7)
Ru—Si—C(18)	116.1(6)	Si—N(1)—C(19)	173.1(15)

^a Where appropriate, parameters for the minor rotational isomer are also listed.

Ru—Si distances in the related silyls **1** and **4**. Also, note that the Ru—Si distance in **13** is just as short as the Ru—Si distance in the silylene complex Cp*(PMe₃)₂Ru=Si[S(Tol-*p*)] [Os(CO)₄], however the latter bond length is probably elongated somewhat by steric pressure. The acetonitrile adducts **12** and **15** also possess comparatively short Ru—Si bond lengths, although the errors in the distances for **15** make comparisons with this structure rather meaningless. The Ru—Si distance in **12**, 2.33 Å, is substantially longer than the Ru=Si double bond distance of 2.24 Å in [Cp*(PMe₃)₂Ru=SiMe₂]B(C₆F₅)₄, and also significantly longer than the corresponding distance in **13** (2.28 Å). The latter observation could be interpreted to mean that S(Tol-*p*) substituents at silicon stabilize a silylene complex more than phenyl substituents. However, this postulate is not supported by the Si···NCMe distances, which imply formation of a stronger

adduct with {Cp*(PMe₃)₂Ru=Si[S(Tol-*p*)]₂}⁺ compared to [Cp*(PMe₃)₂Ru=SiR₂]⁺ (R = Ph, Me). For comparison, note that the Si···N dative-bond distance in [Pr₃Si(NCMe)]⁺[Br₅CB₉H₅]⁻ is 1.82(2) Å,^{14a} and the Si···N distance in Me₃Si(pyr)⁺ is 1.86 Å.^{14c}

The degree to which a “no-bond” silylene-like resonance form (**B**) contributes to the ground state of a silylene adduct can be estimated by the summation of angles at silicon, ignoring the Si—N bond. The silylene complexes in Table 9, Cp*(PMe₃)₂Ru=Si[S(Tol-*p*)] [Os(CO)₄] and [Cp*(PMe₃)₂Ru=SiMe₂]BPh₄, have bond angles at silicon which sum to 360°, reflecting *sp*² hybridization.

As expected (Table 9), the summations for **12**, **13**, and **15** are intermediate between the tetrahedral (329°) and trigonal (360°) values. Surprisingly, the least silylene-like structure is that of **13** (339°), followed by **15** (344°) and then **12** (352°). In fact, the

Table 9. Comparison of structural parameters for Cp*(PMe₃)₂Ru silyl and silylene complexes

Structure	d(Ru—Si) (Å)	d(Si···base) (Å)	Σ(angles @ Si) ^a (°)	⟨R—Si—R ^b ⟩ (°)	Ref.
Cp*(PMe ₃) ₂ RuSi[S(Tol- <i>p</i>)] ₃ (1)	2.350		309–346	102.9 ^c	This work
Cp*(PMe ₃) ₂ RuSi[S(Tol- <i>p</i>)] ₂ OTf (4)	2.306	1.855	334	97.8	This work
{Cp*(PMe ₃) ₂ RuSi[S(Tol- <i>p</i>)] ₃ (NCMe)}BPPh ₄ (13)	2.284	1.866	339	114.9	This work
Cp*(PMe ₃) ₂ Ru=Si[S(Tol- <i>p</i>)] ₃ [Os(CO) ₄]	2.286		360	113.2	19
Cp*(PMe ₃) ₂ RuSiHPh ₂	2.387		342 ^d	100.5	6a
Cp*(PMe ₃) ₂ RuSiPh ₂ OTf	2.349	1.853	341	103.7	6a
[Cp*(PMe ₃) ₂ RuSiPh ₂ (NCMe)]BPPh ₄ (12)	2.328	1.932	352	102.2	6a
[Cp*(PMe ₃) ₂ RuSiMe ₂ (NCMe)]BPPh ₄ (15)	2.258, 2.190	1.963	344	102.8	This work
[Cp*(PMe ₃) ₂ Ru=SiMe ₂]BPPh ₄	2.238		359	99.7	17

^a Summation of bond angles at silicon, ignoring the bond to the donor atom of the Lewis base (NCMe or OTf⁻).

^b The bond angle at silicon that does not involve Ru or the donor atom of the Lewis base (NCMe or OTf⁻), except where indicated.

^c Average of S—Si—S angles.

^d This value is obtained by regarding the hydride group on silicon as the Lewis base.

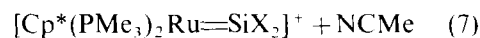
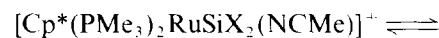
value for **13** is in line with summations that can be calculated for tetrahedral silicon centers bound to ruthenium (Table 9).

It has been noted previously that germylene and stannylene complexes L_nM=EX₂ (E = Ge, Sn) tend to have X—M—X angles that are contracted relative to what is observed for similar carbene complexes. This can be explained by decreasing steric hindrance as the covalent radius of E increases, or to an electronic effect resulting from concentration of *s*-character into the M=E bond.²⁷ The analogous angles for related silicon compounds are listed in Table 9. As can be seen, this angle approaches 100° in many cases, but does not necessarily correlate with silylene character. Interestingly, the bond angles in free dihalosilylenes are *ca* 103°. ²⁸

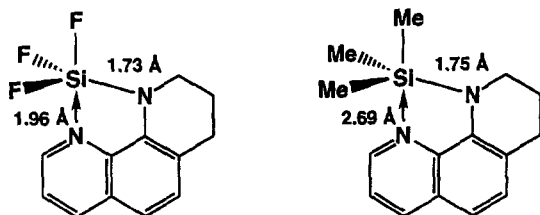
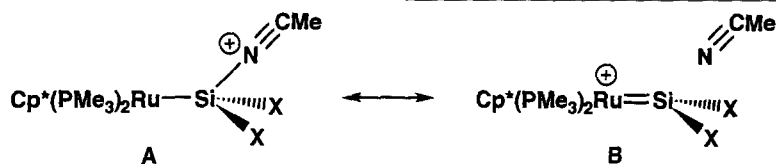
Overall, the structural parameters for the complexes in Table 9 suggest that the S(Tol-*p*) derivative (**13**) has less silylene character than **12** and **15**, as indicated by the summation of angles at silicon and by the Si···N distances. The Ru—Si distances might suggest otherwise, but for various reasons (*vide supra*) this indicator is less reliable. It should be noted, however, that Si···N dative-bond distances can be very sensitive to the electronegativity of substituents at silicon,^{29a} as demonstrated by the pentacoordinate structures.^{29b,c} This example suggests that the difference in Si—N bond lengths observed for **12**, **13**, and **15** might be attributed to the difference in electronegativities for the substituents S(Tol-*p*) vs Ph, Me.

Dynamic studies on acetonitrile exchange in base-stabilized silylene complexes **12–15**

Our previous studies with **12** established that the coordinated acetonitrile exchanges rapidly with free acetonitrile via the equilibrium of eq. (7) (X = Ph). Kinetic studies clearly point to a dissociative mechanism, and intermediacy of the base-free silylene complex [Cp*(PMe₃)₂Ru=SiPh₂]⁺.^{6a} The exchange kinetics were determined by line-shape analyses of



the ¹H NMR spectra. The independence of the rate of exchange on acetonitrile concentration, and the positive entropy of activation (14 ± 1 eu) constitute the evidence for the dissociative nature of the exchange. Significantly, this mechanism and the high rate of acetonitrile dissociation implied that the intermediate silylene complex was relatively stable. We were therefore encouraged to pursue the isolation of [Cp*(PMe₃)₂Ru=SiPh₂]⁺, which was eventually successful.¹⁷



The rate of the acetonitrile dissociation, and the accompanying activation parameters, reflect the stability of the base-free silylene complex relative to its acetonitrile adduct (assuming that significant Si···N bond rupture has occurred in the transition state). With this in mind, we examined the kinetics for acetonitrile dissociation in adducts **13–15**. Comparison of the results for **12–15** then allows an evaluation of the relative stabilizing abilities of substituents at silicon toward a base-free ruthenium silylene complex.

The exchange of bound with free acetonitrile in **13–15** was followed by variable temperature ^1H NMR spectroscopy, and was found to exhibit kinetic behavior analogous to that for **12**. In each case, the room temperature spectrum exhibits a single peak for acetonitrile, which broadens and separates into two peaks as the temperature is lowered. Analysis of this coalescence behavior by line-shape simulations provided reaction rates, from which activation parameters were extracted (Table 10). Activation parameters could not be accurately defined for the fastest exchange involving **13**, since the slow exchange region was not accessible because

of the low coalescence temperature of -75°C (therefore reliable rate constants are available for only a small temperature range, *ca* 20°C). The free energy of activation for this exchange was determined simply from the coalescence temperature.³⁰ The entropies of activation for these reactions are similar, and the positive values are consistent with a dissociative mechanism for acetonitrile exchange. The rates and activation parameters are ordered such that the silylene-stabilizing influences of the substituents decrease according to $\text{S}(\text{Tol-}p) > \text{O}(\text{Tol-}p) > \text{Me} > \text{Ph}$. This trend is consistent with the known stabilities of isolated silylene complexes in solution.^{16,17}

CONCLUSIONS

The synthetic methods described in this study have proven quite versatile in the synthesis of new silyl, base-stabilized silylene, and silylene complexes of $\text{Cp}^*(\text{PMe}_3)_2\text{Ru}$. Triflate(silyl) derivatives are in general readily obtained from chloro(silyl), thiolato(silyl), or alkoxy(silyl) complexes by reaction with Me_3SiOTf . The triflate(silyl) complexes have short Ru—Si bonds that probably have some multiple bond character, and very weak Si—O(triflate) bonds. The lability of the triflate groups in these compounds has proven particularly valuable for elaborating the chemistry of the metal-bound silicon atom via substitution reactions. This lability is such that the triflate derivatives may serve as synthetic precursors for the base-free silylene com-

Table 10. Comparison of activation parameters for acetonitrile exchange in complexes **12–15**

$\text{Cp}^*(\text{PMe}_3)_2\text{RuSiX}_2(\text{NCMe})^+$	T_c^a ($^\circ\text{C}$)	ΔH^\ddagger (kcal mol^{-1})	ΔS^\ddagger (eu)	ΔG^\ddagger^b (kcal mol^{-1})
R = S(Tol- <i>p</i>)	-75 ± 3			8.8 ± 0.2
R = O(Tol- <i>p</i>)	-55 ± 1	12.8 ± 0.5	13 ± 2	10.1 ± 0.7
R = Me	-38 ± 1	14.3 ± 0.2	15 ± 1	11.3 ± 0.3
R = Ph ^c	-30 ± 1	14.5 ± 0.2	14 ± 1	11.7 ± 0.2

^a Coalescence temperature.

^b At -75°C .

^c Ref. 6a.

plexes in polar solvents, in which the triflate groups dissociate reversibly.¹⁶

Displacement of the triflate group in complexes of the type $\text{Cp}^*(\text{PMe}_3)_2\text{RuSiX}_2\text{OTf}$ provides an important, and relatively general, route to base-stabilized and base-free silylene complexes. However, this method has so far been unsuccessful with H, OH, or Cl substituents at silicon. In some respects, the acetonitrile adducts $[\text{Cp}^*(\text{PMe}_3)_2\text{RuSiX}_2(\text{NCMe})]^+$ appear to be more silylene-like than their triflate precursors, although neither type of complex has significant silylene character, as indicated by ²⁹Si NMR and X-ray structural data. Both types of complexes may serve as sources for the base-free silylene in solution, but in general the base adducts are less stable to decomposition and thus less convenient synthetically.

Decompositions of the $[\text{Cp}^*(\text{PMe}_3)_2\text{RuSiX}_2(\text{NCMe})]^+$ adducts occur principally via loss of the silylene fragment. Given the strong interest in possible silylene-transfer reactions that might occur from transition-metal silylene complexes,⁴ we have studied these reactions in detail. So far, we have yet to discover a thermal silylene extrusion reaction which is very clean with respect to formation of both ruthenium- and silicon-containing products. Most disconcerting has been our inability to establish the fate of the lost silylene fragments. Various well-established silylene trapping agents³¹ have not intercepted silylenes in these thermolyses, and other potential silylene-derived species such as *cyclo*-(SiMe₂)₆³² do not form in significant quantities. Interestingly, related observations have been made for the photochemical degradation of $\text{Cp}(\text{CO})_2\text{FeSiR}_2\text{SiR}'_3$ complexes via the stoichiometric loss of silylenes.³³ Given the relevance of transition metal-mediated silylene transfers,⁴ further examination of this problem is clearly warranted.

For the $\text{Cp}^*(\text{PMe}_3)_2\text{RuSiX}_2(\text{NCMe})]^+$ complexes discussed here, different mechanisms for silylene loss appear to operate, depending upon the nature of the X group. This is suggested by the fact that excess acetonitrile accelerates the decomposition of **13**, but stabilizes **15** toward decomposition in solution. One explanation for this behavior is that **15** decomposes via the base-free complex $[\text{Cp}^*(\text{PMe}_3)_2\text{Ru}=\text{SiMe}_2]^+$, while **13** decomposes principally via dissociative loss of the silylene adduct $\text{Si}(\text{STol-}p)_2(\text{NCMe})$. Consistent with this (but also with a mechanism involving fast but reversible dissociation of $:\text{Si}[\text{S}(\text{Tol-}p)]_2$), the decomposition of **13** in the presence of excess NCMe is much faster than the decomposition of $\{\text{Cp}^*(\text{PMe}_3)_2\text{Ru}=\text{Si}[\text{S}(\text{Tol-}p)]_2\}\text{BPh}_4$ in the absence of acetonitrile. For comparison, in dichloromethane $[\text{Cp}^*(\text{PMe}_3)_2\text{Ru}=\text{SiMe}_2]\text{B}(\text{C}_6\text{F}_5)_4$ decom-

poses at room temperature with a half-life of *ca* 7 h.¹⁷ These preliminary results suggest that at least in some cases, the chemistry of base-stabilized silylene complexes can differ significantly from that of the corresponding base-free silylene complex.

Examination of the structures of **12**, **13**, and **15** reveal pyramidal silicon, and marginal evidence for "silylene character". Detailed comparisons of the three structures provide ambiguous answers to the question of whether Ph, Me, or S(Tol-*p*) groups impart more silylene character to the complex. However, the balance of the structural data indicates that **12** is the most, and **13** the least, silylene-like, particularly since the silicon center in the latter complex is most pyramidal. Thus, based on structural data alone, one might predict that $[\text{Cp}^*(\text{PMe}_3)_2\text{Ru}=\text{SiPh}_2]^+$ would be more stable (and more synthetically accessible) than $\{\text{Cp}^*(\text{PMe}_3)_2\text{Ru}=\text{Si}[\text{S}(\text{Tol-}p)]_2\}^+$.

This is clearly not the case. Not only is the triflate derivative easier to prepare, it is more thermally stable. As described above, we have also used a method based on the kinetics of acetonitrile dissociation from $[\text{Cp}^*(\text{PMe}_3)_2\text{RuSiX}_2(\text{NCMe})]^+$ complexes to gauge the stabilizing influence of silylene substituents. This method indicates that the ordering of stabilizing influences is: S(Tol-*p*) > O(Tol-*p*) > Me > Ph, and in our opinion this ordering is reliable. Note that Zybail has suggested a somewhat different "ligand stabilization capacity gradation" of O > S ≫ C, based on structural and spectroscopic data on $(\text{CO})_5\text{FeSiX}_2(\text{HMPA})$ complexes.^{5d}

The ordering observed in our system appears to reflect π-donating abilities for the substituents. On the basis of *ab initio* calculations, Apeloig and coworkers concluded that —SH and —OH have similarly strong π-donating and stabilizing effects as substituents in silylenium ions.³⁴ Also, molecular orbital calculations based on the structure of $[\textit{trans}-(\text{PCy}_3)(\text{H})\text{Pt}=\text{Si}(\text{SEt})_2]^+$ indicated that the silylene ligand gains much more stability from π-bonding to sulfur than from *d*_π-*p*_π donation from platinum.¹⁸ The stabilizing influences of the Me and Ph groups are very similar (Table 10), and any differences between them are probably due mostly to steric effects.

The apparently conflicting conclusions which appear to arise from the structural *vs* the dynamic studies on $[\text{Cp}^*(\text{PMe}_3)_2\text{RuSiX}_2(\text{NCMe})]^+$ adducts appear to suggest that the more stable silylene complexes form stronger adducts with a Lewis base like acetonitrile, resulting in a more pyramidalized silicon center. Therefore the substituents which stabilize silylene ligands the most also give rise to the strongest silicon–Lewis base interactions. This sug-

gests that both silylene complexes and their adducts may be stabilized by a more Lewis acidic silicon center. Thus, a more acidic silicon center could act as a better π -acid for forming strong π -bonds to ruthenium and/or sulfur π -donors or, alternatively, for interaction with a Lewis base. The coordination of acetonitrile to $\{\text{Cp}^*(\text{PMe}_3)_2\text{Ru}=\text{Si}[\text{S}(\text{Tol-}p)]_2\}^+$ appears to disrupt strong sulfur-silicon π -bonding interactions that significantly stabilize the silylene ligand.

Synthetic efforts to obtain a wider range of silicon substituents for isolated base-free silylene complexes are continuing, in attempts to correlate substituent effects with chemical and physical properties for the silylene complexes.

EXPERIMENTAL

All manipulations were performed under an atmosphere of nitrogen using Schlenk techniques and/or a Vacuum Atmospheres glovebox. Dry, oxygen-free solvents were employed throughout. Glassware was flame- or oven-dried before use. Elemental analyses were performed by Pascher Analytical Laboratories or Desert Analytics. Infrared spectra were recorded on a Perkin-Elmer 1330 infrared spectrometer. NMR spectra were obtained with a GE QE-300 instrument at 300 MHz (^1H), 75.5 MHz (^{13}C), 121.5 MHz (^{31}P), and 59.6 MHz (^{29}Si). Conductivity measurements were determined on solutions of *ca* 0.004 M concentration. The compound $\text{Cp}^*(\text{PMe}_3)_2\text{RuCH}_2\text{SiMe}_3$ was prepared according to the literature procedure.³⁵ Alkoxy and thioalkoxysilanes were obtained by standard methods, via reaction of the corresponding chlorosilane with an alcohol or thiol in the presence of NEt_3 .³⁶

$\text{Cp}^*(\text{PMe}_3)_2\text{RuSi}[\text{S}(\text{Tol-}p)]_3$ (1)

Toluene (7 cm³), $\text{Cp}^*(\text{PMe}_3)_2\text{RuCH}_2\text{SiMe}_3$ (1.75 g, 3.68 mmol), and $\text{HSi}[\text{S}(\text{Tol-}p)]_3$ (1.53 g, 3.84 mmol) were combined in a flask. The closed and tightly secured flask was heated to 100°C for 6 h. After removing the volatile material *in vacuo*, the product was crystallized from a 1:1 dichloromethane/diethyl ether mixture at -78°C. Yield 85% (2.46 g). Anal. Found: C, 56.2; H, 7.00. Anal. Calc. for $\text{C}_{37}\text{H}_{54}\text{P}_2\text{RuS}_3\text{Si}$: C, 56.6; H, 6.87. M.p. 219–228°C (dec). ^1H NMR (23°C, benzene-*d*₆): δ 1.33 (virtual t, 18 H, PMe_3), 1.81 (s, 15 H, Cp^*), 2.05 (s, 9 H, $\text{SC}_6\text{H}_4\text{Me}$), 6.73 (d, $J = 8$ Hz, 6 H, $\text{SC}_6\text{H}_4\text{Me}$), 7.61 (d, $J = 8$ Hz, 6 H, $\text{SC}_6\text{H}_4\text{Me}$). ^{13}C NMR (23°C, dichloromethane-*d*₂): δ 12.23 (q, $J_{\text{CH}} = 127$ Hz, C_5Me_5), 21.09 (q, $J_{\text{CH}} = 126$ Hz, $\text{SC}_6\text{H}_4\text{Me}$), 24.36 (qt, $J_{\text{CH}} = 124$ Hz, $J_{\text{CP}} = 15$ Hz,

PMe_3), 95.41 (s, C_5Me_5), 128.77 (d, $J_{\text{CH}} = 156$ Hz, $\text{SC}_6\text{H}_4\text{Me}$), 134.20 (d, $J_{\text{CH}} = 161$ Hz, $\text{SC}_6\text{H}_4\text{Me}$), 134.57 (s, $\text{SC}_6\text{H}_4\text{Me}$), 134.98 (s, $\text{SC}_6\text{H}_4\text{Me}$). $^{31}\text{P}\{^1\text{H}\}$ NMR (23°C, dichloromethane-*d*₂): δ 2.23. $^{29}\text{Si}\{^1\text{H}\}$ NMR (23°C, dichloromethane-*d*₂): δ 49.03 (t, $J_{\text{SiP}} = 34$ Hz). IR (Nujol, CsI, cm⁻¹): 1485 s, 1295 w, 1276 m, 1180 w, 1082 w, 1017 m, 952 w, 935 s, 808 s, 795 s, 721 m, 680 w. Equivalent conductance = 0.2 mho cm² equiv⁻¹ (23°C in dichloromethane).

$\text{Cp}^*(\text{PMe}_3)_2\text{RuSi}[\text{O}(\text{Tol-}p)]_3$ (2)

Toluene (15 cm³) was added to $\text{Cp}^*(\text{PMe}_3)_2\text{RuCH}_2\text{SiMe}_3$ (1.38 g, 3.9 mmol) and $\text{HSi}[\text{O}(\text{Tol-}p)]_3$ (1.69 g, 3.5 mmol) and the resulting mixture was then stirred with heating (90°C) in a closed flask *in vacuo*, the precipitate was washed with 2×5 cm³ of pentane at -78°C, and then with 2×10 cm³ of additional pentane (0°C) leaving 1.5 g of a light yellow precipitate. Yield 52%. Anal. Found: C, 60.1; H, 7.54. Anal. Calc. for $\text{C}_{37}\text{H}_{54}\text{O}_3\text{P}_2\text{RuSi}$: C, 60.2; H, 7.38. M.p. 194–199°C (dec). ^1H NMR (benzene-*d*₆, 23°C): δ 1.35 (vir t, 18 H, PMe_3), 1.73 (s, 15 H, C_5Me_5), 2.07 (s, 9 H, $\text{C}_6\text{H}_4\text{Me}$), 6.89 (d, $J = 8$ Hz, 6 H, $\text{C}_6\text{H}_4\text{Me}$), 7.15 (d, $J = 8$ Hz, 6 H, $\text{C}_6\text{H}_4\text{Me}$). $^{13}\text{C}\{^1\text{H}\}$ NMR (benzene-*d*₆, 23°C): δ 11.98 (C_5Me_5), 20.49 ($\text{C}_6\text{H}_4\text{Me}$), 24.25 (vir t, PMe_3), 93.92 (C_5Me_5), 120.40, 128.43, 129.80, 130.05 (aryl carbons). $^{31}\text{P}\{^1\text{H}\}$ NMR (benzene-*d*₆, 23°C): δ 7.81. $^{29}\text{Si}\{^1\text{H}\}$ NMR (benzene-*d*₆, 23°C): δ -1.22 (t, $J_{\text{SiP}} = 42$ Hz). IR (Nujol, CsI, cm⁻¹): 1612 m, 1513 s, 1503 s, 1288 s, 1248 s, 1166 w, 1103 w, 968 w, 940 m, 930 m, 898 s, 818 m, 788 m, 704 w, 663 w, 627 w, 615 w.

$\text{Cp}^*(\text{PMe}_3)_2\text{RuSiMe}_2[\text{S}(\text{Tol-}p)]$ (3)

Toluene (30 cm³), $\text{Cp}^*(\text{PMe}_3)_2\text{RuCH}_2\text{SiMe}_3$ (5.38 g, 11.3 mmol) and $\text{HSiMe}_2[\text{S}(\text{Tol-}p)]$ (2.12 g, 11.3 mmol) were stirred at 100°C in a closed flask for 5 h. After removing the volatile material *in vacuo*, the precipitate was washed with pentane (2×10 cm³) leaving 5.7 g of a light yellow precipitate. Yield 88%. Anal. Found: C, 52.8; H, 7.82. Anal. Calc. for $\text{C}_{25}\text{H}_{46}\text{P}_2\text{RuSSi}$: C, 52.7; H, 8.14. M.p. 169–173°C (dec). ^1H NMR (benzene-*d*₆, 23°C): δ 0.63 (s, 6 H, SiMe_2), 1.22 (vir t, 18 H, PMe_3), 1.78 (s, 15 H, C_5Me_5), 2.10 (s, 3 H, $\text{C}_6\text{H}_4\text{Me}$), 7.00 (d, $J = 8$ Hz, 2 H, $\text{C}_6\text{H}_4\text{Me}$), 7.68 (d, $J = 8$ Hz, 2 H, $\text{C}_6\text{H}_4\text{Me}$). $^{13}\text{C}\{^1\text{H}\}$ NMR (benzene-*d*₆, 23°C): δ 11.27 (SiMe_2), 12.33 (C_5Me_5), 21.09 ($\text{C}_6\text{H}_4\text{Me}$), 24.15 (vir t, PMe_3), 94.08 (C_5Me_5), 129.04, 134.36, 135.40, 135.89 (aryl carbons). $^{31}\text{P}\{^1\text{H}\}$ NMR (benzene-*d*₆, 23°C): δ 5.37. $^{29}\text{Si}\{^1\text{H}\}$

NMR (benzene- d_6 , 23°C): δ 50.19 (t, $^2J_{\text{SiP}} = 42$ Hz). IR (Nujol, CsI, cm^{-1}): 1302 w, 1296 w, 1275 m, 1224 w, 1088 w, 1020 m, 955 s, 938 s, 833 m, 809 m, 780 s, 702 m, 620 m, 612 w, 409 m.

Cp*(PMe₃)₂RuSi[S(Tol-p)]₂OTf (4)

Me₃SiOTf (1.38 cm³, 7.56 mmol) was added to a benzene (100 cm³) solution of **1** (5.40 g, 6.87 mmol). The resulting solution was stirred at 45°C for 12 h while precipitation of **4** occurred. After the volatile material was removed, the product was crystallized from a 1 : 1 dichloromethane/diethyl ether mixture at -78°C. Yield 2.58 g (46%). Anal. Found: C, 45.8; H, 5.95. Anal. Calc. for C₃₁H₄₇F₃O₃P₂RuS₃Si: C, 45.9; H, 5.83. M.p. 168–178°C (dec). ¹H NMR (23°C, dichloromethane- d_2): δ 1.37 (virtual t, 18 H, PMe₃), 1.86 (s, 15 H, Cp*), 2.28 (s, 6 H, SC₆H₄Me), 6.97 (d, $J = 8$ Hz, 4 H, SC₆H₄Me), 7.37 (d, $J = 8$ Hz, 4 H, SC₆H₄Me). ¹³C{¹H} NMR (23°C, dichloromethane- d_2): δ 11.65 (s, C₅Me₅), 21.16 (s, SC₆H₄Me), 24.06 (t, $J_{\text{CP}} = 16$ Hz, PMe₃), 95.66 (s, C₅Me₅), 129.28, 130.79, 135.23, 136.74 (SC₆H₄Me). ³¹P{¹H} NMR (23°C, dichloromethane- d_2): δ 0.66. ²⁹Si{¹H} NMR (23°C, dichloromethane- d_2): δ 77.14 (t, $J_{\text{SiP}} = 36$ Hz). IR (Nujol, CsI, cm^{-1}): 1488 m, 1367 s $\nu(\text{SO}_3)$, 1238 m, 1203 s, 1177 s, 1154 m, 958 m, 940 m, 927 s, 819 w, 808 w, 718 w, 631 m. Equivalent conductance = 8 mho cm² equiv⁻¹ (23°C in dichloromethane); 133 mho cm² equiv⁻¹ (23°C in acetonitrile).

Cp*(PMe₃)₂RuSi[O(Tol-p)]₂OTf (5)

Trimethylsilyl triflate (0.10 cm³, 0.56 mmol) was syringed into a diethyl ether (10 cm³) solution of **2**, and the resulting solution was stirred for 16 h. The solution was filtered and cooled to -35°C, resulting in 0.23 g of yellow crystals. Yield 88%. Anal. Found: C, 48.0; H, 5.95. Anal. Calc. for C₃₁H₄₇F₃O₅P₂RuSSi: C, 47.7; H, 6.07. M.p. 182–186°C (dec). ¹H NMR (dichloromethane- d_2 , 23°C): δ 1.52 (vir t, 18 H, PMe₃), 1.83 (s, 15 H, C₅Me₅), 2.23 (s, 6 H, C₆H₄Me), 6.77 (d, $J = 8$ Hz, 4 H, C₆H₄Me), 6.91 (d, $J = 8$ Hz, 4 H, C₆H₄Me). ¹³C{¹H} NMR (dichloromethane- d_2 , 23°C): δ 10.64 (C₅Me₅), 19.68 (C₆H₄Me), 22.80 (vir t, PMe₃), 93.95 (C₅Me₅), 119.21, 128.70, 129.41, 152.15 (aryl carbons). ³¹P{¹H} NMR (dichloromethane- d_2 , 23°C): δ 4.60. ²⁹Si{¹H} NMR (dichloromethane- d_2 , 23°C): δ -0.01 (t, $^2J_{\text{SiP}} = 45$ Hz). IR (Nujol, CsI, cm^{-1}): 1609 m, 1510 s, 1358 s $\nu(\text{SO}_3)$, 1283 w, 1276 m, 1263 m, 1238 m, 1197 s, 1171 w, 1155 w, 981 m, 956 m, 913 m, 903 s, 821 m, 628 m.

Cp*(PMe₃)₂RuSiMe₂OTf (6)

Trimethylsilyl triflate (2.0 cm³, 11 mmol) was added to a diethyl ether (40 cm³)/dichloromethane (10 cm³) solution of **3** (5.7 g, 10 mmol). The resulting solution was stirred for 18 h and then the volatile material was removed *in vacuo*, leaving a yellow precipitate. The product was extracted into 30 cm³ of dichloromethane and the resulting solution was filtered away from undissolved solids. After adding 20 cm³ of diethyl ether and cooling to -78°C, crystals formed, and these were isolated to give 5.66 g of a light yellow product. Yield 95%. Anal. Found: C, 38.3; H, 6.55. Anal. Calc. for C₁₉H₃₉F₃O₃P₂RuSSi: C, 38.3; H, 6.60. M.p. 235–241°C (dec). ¹H NMR (benzene- d_6 , 23°C): δ 0.68 (s, 6 H, SiMe₂), 1.37 (vir t, 18 H, PMe₃), 1.77 (t, $J_{\text{HP}} = 1$ Hz, 15 H, C₅Me₅). ¹³C{¹H} NMR (benzene- d_6 , 23°C): δ 11.85 (C₅Me₅), 12.81 (SiMe₂), 23.91 (vir t, PMe₃), 94.17 (C₅Me₅). ³¹P{¹H} NMR (benzene- d_6 , 23°C): δ 5.50. ²⁹Si{¹H} NMR (benzene- d_6 , 23°C): δ 133.29 (t, $^2J_{\text{SiP}} = 33$ Hz). IR (dichloromethane, KBr, cm^{-1}): 2952 m, 2900 s, 1477 m, 1458 w, 1424 m, 1376 m, 1350 s, 1299 m, 1265 m, 1236 s, 1195 s, 1158 s, 1063 w, 1028 m.

Cp*(PMe₃)₂RuSi[S(Tol-p)](OTf)₂ (7)

Me₃SiOTf (11 cm³, 60 mmol) was added to a dichloromethane (250 cm³) solution of **1** (13.0 g, 16.6 mmol), and the resulting solution was stirred for 4 days. After adding diethyl ether and cooling to -35°C, light yellow crystals formed. A second crop was obtained by concentration and cooling of the mother liquors to give a total yield of 10.8 g (78%). Anal. Found: C, 35.8; H, 4.78. Anal. Calc. for C₂₅H₄₀F₆O₆P₂RuS₃Si: C, 35.8; H, 4.81. M.p. 192–197°C (dec). ¹H NMR (23°C, dichloromethane- d_2): δ 1.50 (virtual t, 18 H, PMe₃), 1.91 (s, 15 H, Cp*), 2.31 (s, 3 H, SC₆H₄Me), 7.05 (d, $J = 8$ Hz, 2 H, SC₆H₄Me), 7.38 (d, $J = 8$ Hz, 2 H, SC₆H₄Me). ¹³C{¹H} NMR (23°C, dichloromethane- d_2): δ 11.32 (s, C₅Me₅), 21.22 (s, SC₆H₄Me), 23.63 (t, $J_{\text{CP}} = 16$ Hz, PMe₃), 96.33 (s, C₅Me₅), 129.02, 129.29, 135.31, 137.15 (SC₆H₄Me). ³¹P{¹H} NMR (23°C, dichloromethane- d_2): δ 0.26. ²⁹Si{¹H} NMR (23°C, dichloromethane- d_2): δ 37.10 (t, $J_{\text{SiP}} = 39$ Hz). IR (Nujol, CsI, cm^{-1}): 1485 w, 1365 s, 1239 m, 1219 s, 1202 s, 1187 s, 1143 m, 1017 w, 967 m, 948 s, 904 m, 853 w, 805 w, 718 w, 632 s. Equivalent conductance = 3 mho cm² equiv⁻¹ (23°C in dichloromethane); 131 mho cm² equiv⁻¹ (23°C in acetonitrile).

Cp*(PMe₃)₂RuSi[S(Tol-p)]₂H (8)

LiHBEt₃ (0.62 cm³ of a 1.0 M tetrahydrofuran solution, 0.62 mmol) was added to a toluene solu-

tion (40 cm³) of **4** (0.50 g, 0.62 mmol), and the resulting solution was stirred for 2 h. All volatile material was removed *in vacuo*, and the precipitate was extracted with toluene (2 × 10 cm³). After concentration and cooling of the toluene extract to -35°C, light yellow crystals formed, which were isolated by filtration (0.20 g). Yield 50%. Anal. Found: C, 54.3; H, 7.17. Anal. Calc. for C₃₀H₄₈P₂RuS₂Si: C, 54.3; H, 7.29. ¹H NMR (benzene-*d*₆, 23°C): δ 1.23 (vir t, 18 H, PMe₃), 1.87 (t, *J*_{HP} = 1 Hz, 15 H, C₅Me₅), 2.06 (s, 6 H, C₆H₄Me), 6.17 (t, *J*_{HP} = 4 Hz, 1 H, SiH), 6.77 (d, *J* = 8 Hz, 4 H, C₆H₄Me), 7.43 (d, *J* = 8 Hz, 4 H, C₆H₄Me). ¹³C{¹H} NMR (benzene-*d*₆, 23°C): δ 12.15 (C₅Me₅), 21.04 (C₆H₄Me), 22.42 (vir t, PMe₃), 94.18 (C₅Me₅), 128.99, 133.87, 134.04, 136.91 (aryl carbons). ³¹P{¹H} NMR (benzene-*d*₆, 23°C): δ 3.42. ²⁹Si NMR (benzene-*d*₆, 23°C): δ 67.95 (d of t, ¹*J*_{SiH} = 191 Hz, ²*J*_{SiP} = 31 Hz). IR (Nujol, CsI, cm⁻¹): 2058 m (SiH), 1296 m, 1278 m, 1087 w, 1018 w, 953 s, 938 s, 800 s, 729 m, 713 w, 702 w, 616 m, 455 m, 432 m.

Cp*(PMe₃)₂RuSi[S(Tol-*p*)](H)(OTf) (**9**)

Trimethylsilyl triflate (0.050 cm³, 0.27 mmol) was syringed into a diethyl ether (3 cm³) dichloromethane (1 cm³) solution of Cp*(PMe₃)₂RuSi[S(Tol-*p*)]₂H (0.180 g, 0.27 mmol), and the resulting solution was stirred for 16 h. The solution was then filtered and the filtrate was concentrated to 1 cm³. Cooling to -35°C produced yellow crystals, which were isolated by filtration and washed with pentane (2 cm³). Yield 0.12 g (62%). Anal. Found: C, 42.1; H, 5.94. Anal. Calc. for C₂₄H₄₁F₃O₃P₂RuS₂Si: C, 41.8; H, 5.99. ¹H NMR (dichloromethane-*d*₂, 23°C): δ 1.45 (d, *J*_{HP} = 8 Hz, 18 H, PMe₃), 1.87 (t, *J*_{HP} = 2 Hz, 15 H, C₅Me₅), 2.30 (s, 3 H, C₆H₄Me), 6.29 (m, 1 H, SiH), 7.03 (d, *J* = 8 Hz, 2 H, C₆H₄Me), 7.36 (d, *J* = 8 Hz, 2 H, C₆H₄Me). ¹³C NMR (dichloromethane-*d*₂, 23°C): δ 11.62 (q, *J* = 127 Hz, C₅Me₅), 21.03 (q, *J* = 122 Hz, C₆H₄Me), 22.2 (m, PMe₃), 94.80 (C₅Me₅), 129.42 (d, *J* = 152 Hz), 133.35 (d, *J* = 160 Hz), 134.45, 135.98 (aryl carbons). ³¹P{¹H} NMR (dichloromethane-*d*₂, 23°C): δ 2.16 (d, *J*_{PP} = 38 Hz), 3.54 (d, *J*_{PP} = 38 Hz). ²⁹Si NMR (benzene-*d*₆, 23°C): δ 88.81 (d of t, ¹*J*_{SiH} = 196 Hz, ²*J*_{SiP} = 36 Hz). IR (Nujol, CsI, cm⁻¹): 2088 m (SiH), 1378 s, 1355 s, 1283 w, 1239 m, 1203 s, 1190 s, 1157 m, 1084 w, 988 s, 955 s, 939 m, 830 m, 803 w, 715 w, 628 m, 468 m, 414 w, 322 w.

Cp*(PMe₃)₂RuSi[S(Tol-*p*)](OH)(OTf) (**10**)

Degassed H₂O (7.0 μl, 0.39 mmol) was added to a dichloromethane (10 cm³) solution of

Cp*(PMe₃)₂RuSi[S(Tol-*p*)]₂(OTf) (0.30 g, 0.37 mmol). Stirring for 1 h resulted in a cloudy solution. This solution was filtered, and then diethyl ether (4 cm³) was added to the filtrate. The crystals that formed upon cooling to -35°C were isolated by filtration, and washed with diethyl ether (3 cm³) to afford in 0.15 g of product. Yield 58%. Anal. Found: C, 42.5; H, 5.99. Anal. Calc. for C₂₄H₃₁F₃O₄P₂RuS₂Si: C, 40.8; H, 5.86. M.p. 167–173°C (dec). ¹H NMR (dichloromethane-*d*₂, 23°C): δ 1.43 (vir t, 18 H, PMe₃), 1.71 (s, 15 H, C₅Me₅), 2.36 (s, 3 H, C₆H₄Me), 4.78 (t, *J*_{HP} = 7 Hz, 1 H, SiOH), 7.21 (d, *J* = 8 Hz, 2 H, C₆H₄Me), 7.28 (d, *J* = 8 Hz, 2 H, C₆H₄Me). ¹³C{¹H} NMR (dichloromethane-*d*₂, 23°C): δ 10.81 (C₅Me₅), 20.50 (vir t, PMe₃), 21.12 (C₆H₄Me), 93.17 (C₅Me₅), 125.76, 130.23, 130.59, 139.43 (aryl carbons). ³¹P{¹H} NMR (dichloromethane-*d*₂, 23°C): δ -0.60. IR (Nujol, CsI, cm⁻¹): 2438 br m (SiOH), 1292 s, 1278 s, 1248 s, 1221 m, 1152 s, 1029 s, 957 m, 939 m, 850 w, 803 w, 720 w, 633 m.

Cp*(PMe₃)₂RuSiCl₂OTf (**11**) from **4** and HCl

A hydrogen chloride-saturated benzene solution (3 cm³) was syringed into a toluene (50 cm³) solution of **4** (0.01 g, 1.1 mmol), and the resulting mixture was stirred for 5 min. Another 4 cm³ of the hydrogen chloride solution was then added, and stirring was continued for an additional 20 min before nitrogen gas was bubbled through the solution (15 min) to remove excess hydrogen chloride. After removing the volatile material *in vacuo*, the precipitate was washed with pentane (10 cm³) and then extracted into toluene (2 × 15 cm³). Crystallization occurred upon cooling the solution to -35°C; 0.51 g of yellow crystals were isolated by filtration. Yield 75%. Anal. Found: C, 32.4; H, 5.10. Anal. Calc. for C₁₇H₃₃Cl₂F₃O₃P₂RuSSi: C, 32.1; H, 5.23. M.p. 190–204°C (dec). ¹H NMR (dichloromethane-*d*₂, 23°C): δ 1.45 (vir t, 18 H, PMe₃), 1.79 (t, *J*_{HP} = 1 Hz, 15 H, C₅Me₅). ¹³C{¹H} NMR (dichloromethane-*d*₂, 23°C): δ 11.38 (C₅Me₅), 23.03 (vir t, PMe₃), 95.75 (C₅Me₅). ³¹P{¹H} NMR (dichloromethane-*d*₂, 23°C): δ 3.16. ²⁹Si{¹H} NMR (dichloromethane-*d*₂, 23°C): δ 32.92 (t, ²*J*_{SiP} = 45 Hz). IR (Nujol, CsI, cm⁻¹): 1301 w, 1283 w, 1240 m, 1197 br s, 1150 s, 961 m, 936 s, 917 s, 852 w, 719 m, 667 w, 630 m, 509 w, 482 m, 455 m.

Cp*(PMe₃)₂RuSiCl₂OTf (**11**) from Cp*(PMe₃)₂RuSiCl₃ and Me₃SiOTf (**11**)

Trimethylsilyltriflate (7 μl, 0.40 mmol) was added to a benzene-*d*₆ solution of Cp*(PMe₃)₂RuSiCl₃

(0.010 g, 0.019 mmol). The solution was monitored by ^1H and ^{31}P NMR spectroscopy over 12 days, and during this time clean conversion to **11** and Me_3SiCl was observed.

$\{\text{Cp}^*(\text{PMe}_3)_2\text{RuSi}[\text{S}(\text{Tol-p})]_2\text{NCMe}\}\text{BPh}_4$ (**13**)

Compound **4** (0.60 g, 0.74 mmol) was dissolved in a mixture of dichloromethane (30 cm^3) and acetonitrile (0.38 cm^3 , 10 equiv), and the resulting solution was then transferred by cannulae to a flask containing NaBPh_4 (0.51 g, 2 equiv). This solution was stirred for 6 h and was then filtered to remove NaOTf and unreacted NaBPh_4 . Addition of diethyl ether (20 cm^3) and cooling to -35°C resulted in formation of pale yellow crystals. Yield 0.46 g (61%). Anal. Found: C, 65.7; H, 6.93; N, 1.43. Anal. Calc. for $\text{C}_{36}\text{H}_{70}\text{BNP}_2\text{RuS}_2\text{Si}$: C, 65.8; H, 6.90; N, 1.37. M.p. $135\text{--}141^\circ\text{C}$ (dec). ^1H NMR (23 $^\circ\text{C}$, dichloromethane- d_2): δ 1.42 (virtual t, 18 H, PMe_3), 1.67 (s, 3 H, NCMe), 1.89 (s, 15 H, Cp^*), 2.33 (s, 6 H, $\text{SC}_6\text{H}_4\text{Me}$), 6.89 (t, $J = 7$ Hz, 4 H, $\text{SC}_6\text{H}_4\text{Me}$), 7.04 (m, 16 H, $\text{SC}_6\text{H}_4\text{Me}$ and BPh_4), 7.35 (br, 8 H, BPh_4). $^{13}\text{C}\{^1\text{H}\}$ NMR (23 $^\circ\text{C}$, dichloromethane- d_2): δ 0.29 (NCMe), 10.84 (s, C_5Me_5), 20.08 (s, $\text{SC}_6\text{H}_4\text{Me}$), 22.51 (t, $J_{\text{CP}} = 14$ Hz, PMe_3), 95.07 (s, C_5Me_5), 116.77, 121.36, 125.27, 129.34, 130.00, 134.43, 135.38, 137.30 (aryl carbons), 163.50 (q, $J_{\text{CB}} = 49$, ipso BPh_4). $^{31}\text{P}\{^1\text{H}\}$ NMR (23 $^\circ\text{C}$, dichloromethane- d_2): δ -0.96 . ^{29}Si NMR (23 $^\circ\text{C}$, dichloromethane- d_2): δ 58.30 (t, $J_{\text{SiP}} = 39$ Hz). IR (Nujol, Csl , cm^{-1}): 2263 w (NCMe), 1481 w, 1448 w, 1277 w, 1012 w, 951 m, 938 s, 845 w, 807 m, 737 m, 701 s, 662 m.

$\{\text{Cp}^*(\text{PMe}_3)_2\text{RuSi}[\text{O}(\text{Tol-p})]_2\text{NCMe}\}\text{BPh}_4$ (**14**)

Complex **5** (0.44 g, 0.56 mmol) was dissolved in a mixture of dichloromethane (30 cm^3) and acetonitrile (0.29 cm^3 , 10 equiv), and the resulting solution was then transferred by cannulae to a flask containing NaBPh_4 (0.23 g, 1.2 equiv). This solution was stirred for 14 h, and was then filtered. Diethyl ether (30 cm^3) was then added and the solution was cooled to -35°C , resulting in the formation of pale yellow crystals. A second crop was isolated upon addition of more diethyl ether and further cooling. Total yield 0.20 g (36%). Anal. Found: C, 68.0; H, 6.89; N, 1.24. Anal. Calc. for $\text{C}_{54}\text{H}_{67}\text{BNO}_2\text{P}_2\text{RuSi}$: C, 67.9; H, 7.12; N, 1.41. ^1H NMR (dichloromethane- d_2 , 23 $^\circ\text{C}$): δ 1.03 (s, 3 H, NCMe), 1.50 (vir t, 18 H, PMe_3), 1.83 (s, 15 H, C_5Me_5), 2.22 (s, 6 H, $\text{C}_6\text{H}_4\text{Me}$), 6.59 (d, $J = 8$ Hz, 4 H, $\text{C}_6\text{H}_4\text{Me}$), 6.86 (t, $J = 7$ Hz, 4 H, BPh_4), 6.93 (d, $J = 8$ Hz, 4 H, $\text{C}_6\text{H}_4\text{Me}$), 7.01 (t, $J = 7$ Hz, 8 H, BPh_4), 7.35 (m, 8 H, BPh_4). $^{13}\text{C}\{^1\text{H}\}$ NMR

(dichloromethane- d_2 , 23 $^\circ\text{C}$): δ -0.10 (NCMe), 11.61 (C_5Me_5), 20.61 ($\text{C}_6\text{H}_4\text{Me}$), 23.81 (vir t, PMe_3), 95.50 (C_5Me_5), 119.56, 122.11, 126.19, 130.34, 132.10, 136.16, 152.18 (aryl carbons), 164.57 (q, $J_{\text{CB}} = 49$ Hz, ipso carbon of BPh_4). $^{31}\text{P}\{^1\text{H}\}$ NMR (dichloromethane- d_2 , 23 $^\circ\text{C}$): δ 0.94. $^{29}\text{Si}\{^1\text{H}\}$ NMR (dichloromethane- d_2 , 23 $^\circ\text{C}$): δ 14.33 (t, $^2J_{\text{SiP}} = 47$ Hz). IR (dichloromethane, KBr , cm^{-1}): 3027 s, 2991 m, 2973 m, 2900 s, 2311 w (NCMe), 2282 m (NCMe), 1609 w, 1579 m, 1500 vs, 1473 s, 1418 w, 1373 w, 1223 vs, 1167 w.

$[\text{Cp}^*(\text{PMe}_3)_2\text{RuSiMe}_2(\text{NCMe})]\text{BPh}_4$ (**15**)

A mixture of dichloromethane (20 cm^3) and acetonitrile (4.6 cm^3 , 50 equiv) was added to a flask containing **6** (1.04 g, 1.75 mmol) and NaBPh_4 (0.716 g, 1.2 equiv) which had been cooled to 0°C . The resulting heterogeneous mixture was stirred for 1.5 h at 0°C , and then diethyl ether (15 cm^3) was added. The solution was filtered, more diethyl ether (20 cm^3) was added to the filtrate, and the solution was cooled to -20°C resulting in crystallization of 1.04 g of slightly yellow prisms. Yield 74%. Anal. Found: C, 65.2; H, 7.58; N, 1.75. Anal. Calc. for $\text{C}_{43}\text{H}_{62}\text{BNP}_2\text{RuSi}$: C, 65.5; H, 7.74; N, 1.74. M.p. $166\text{--}177^\circ\text{C}$ (dec). ^1H NMR (dichloromethane- d_2 , 23 $^\circ\text{C}$): δ 0.64 (s, 6 H, SiMe_2), 1.36 (vir t, 18 H, PMe_3), 1.45 (s, 3 H, NCMe), 1.76 (t, $J_{\text{HP}} = 1$ Hz, 15 H, C_5Me_5), 6.86 (t, $J = 7$ Hz, 4 H, BPh_4), 7.01 (t, $J = 7$ Hz, 8 H, BPh_4), 7.35 (m, 8 H, BPh_4). $^{13}\text{C}\{^1\text{H}\}$ NMR (dichloromethane- d_2 , 23 $^\circ\text{C}$): δ 11.72 (C_5Me_5), 12.51 (SiMe_2), 23.94 (vir t, PMe_3), 94.60 (C_5Me_5), 122.09, 126.09, 136.13, 164.42 (q, $J_{\text{CP}} = 49$ Hz, ipso carbons on BPh_4). $^{31}\text{P}\{^1\text{H}\}$ NMR (dichloromethane- d_2 , 23 $^\circ\text{C}$): δ 4.65. $^{29}\text{Si}\{^1\text{H}\}$ NMR (dichloromethane- d_2 , 23 $^\circ\text{C}$): δ 110.03 (t, $^2J_{\text{SiP}} = 30$ Hz). IR (dichloromethane, KBr , cm^{-1}): 2965 br s, 2900 s, 2280 m (NCMe), 1578 m, 1475 s, 1419 m, 1374 m, 1299 w, 1279 br w, 1177 w, 1140 m, 1061 w, 1021 m.

$[\text{Cp}^*(\text{PMe}_3)_2\text{RuSiMe}_2(\text{DMAP})]\text{BPh}_4 \cdot 0.5\text{CH}_2\text{Cl}_2$ (**16**)

Dichloromethane (10 cm^3) was added to a flask containing **6** (0.25 g, 0.42 mmol), 4-dimethylaminopyridine (DMAP, 0.41 g, 8 equiv), and NaBPh_4 (0.72 g, 1.2 equiv), and the heterogeneous mixture was stirred for 3 h. The solution was then filtered and the product was precipitated with diethyl ether (*ca* 20 cm^3). The product was washed with 3×7 cm^3 of benzene and was then crystallized from 1 : 1 dichloromethane/diethyl ether (*ca* 5 cm^3), resulting in 0.12 g of light yellow product. Yield 29%. Anal. Found: C, 63.4; H, 7.28; N, 3.05. Anal.

Calc. for $C_{49.5}H_{70}BClN_2P_2RuSi$: C, 63.8; H, 7.60; N, 3.02. 1H NMR (dichloromethane- d_2 , 23°C): δ 0.51 (s, 6 H, $SiMe_2$), 1.44 (vir t, 18 H, PMe_3), 1.63 (t, $J_{HP} = 1$ Hz, 15 H, C_5Me_5), 3.05 (s, 6H, $NC_5H_4NMe_2$), 6.61 (d, $J = 8$ Hz, 2 H, $NC_5H_4NMe_2$), 6.86 (t, $J = 7$ Hz, 4 H, BPh_4), 7.01 (t, $J = 7$ Hz, 8 H, BPh_4), 7.35 (m, 8 H, BPh_4), 8.21 (d, $J = 8$ Hz, 2 H, $NC_5H_4NMe_2$). $^{13}C\{^1H\}$ NMR (dichloromethane- d_2 , 23°C): δ 11.64 (C_5Me_5), 12.47 ($SiMe_2$), 24.21 (vir t, PMe_3), 39.85 ($NC_5H_4NMe_2$), 94.39 (C_5Me_5), 106.84, 122.17, 126.09, 136.22, 145.06, 156.14, 164.42 (q, $J_{CP} = 49$ Hz, ipso carbons on BPh_4). $^{31}P\{^1H\}$ NMR (dichloromethane- d_2 , 23°C): δ 2.93. IR (Nujol, CsI, cm^{-1}): 1622 s, 1550 w, 1303 w, 1281 m, 1224 s, 1147 w, 1063 s, 1020 s, 949 m, 931 s, 819 w, 783 m, 741 m, 727 m, 700 m.

Dynamic NMR studies

The thermocouple in the QE-300 spectrometer's variable temperature unit was calibrated before each run using the chemical shift for neat methanol. A temperature dependence was found for the chemical shift of the bound NCMc in the base-stabilized silylene complexes, and this temperature dependence was accounted for in the simulations. The theoretical line shapes were calculated by a program written in BASIC for Macintosh using expressions derived by Rogers and Woodbrey^{30a} for an uncoupled two site exchange and equations described by Sandström.^{30b} The calculated and experimental spectra were visually compared and the exchange rate was taken as that which produced a simulated spectrum that was the same as the experimental spectrum. The concentration dependencies were determined by monitoring the acetonitrile peak's width at half height as a function of acetonitrile concentration in the slow exchange region.

X-ray structure determinations

Crystal, data collection, and refinement parameters are collected in Tables 1 and 6. Additional details are given in the supplementary material. Crystals were mounted in glass capillaries under nitrogen and flame-sealed. Centering of 25 randomly selected reflections with $15^\circ \leq 2\theta \leq 30^\circ$ provided unit cell data. The selection of the triclinic cell was confirmed by axial photographs. Structures were solved by direct methods (unless stated otherwise) and refined by full-matrix least-squares methods, using the SHELXTL program library (G. Sheldrick; Nicolet (Siemens) Corp., Madison, WI).

For $Cp^*(PMe_3)_2RuSi[S(Tol-p)]_3$ (1). The selection of the triclinic cell was confirmed by axial

photographs. The diffraction data were corrected for Lorentz and polarization effects, and for a slight decay of ca 1% in the intensity of three check reflections. A semi-empirical absorption correction based on the Ψ scan method was employed. All non-hydrogen atoms were refined anisotropically. The hydrogen atoms were placed in idealized, calculated positions [$d(C-H) = 0.96$ Å], with a fixed thermal parameter approximately equal to 1.2 times the isotropic thermal of the attached carbon atom.

For $Cp^*(PMe_3)_2RuSi[S(Tol-p)]_2OTf$ (4). Axial photographs confirmed the lattice assignment as monoclinic. The data was corrected for Lorentz and polarization effects, however no absorption correction was needed. Systematic absences uniquely determined the space group as $P2_1/c$. All non-hydrogen atoms were refined anisotropically. The hydrogen atoms were calculated and fixed in idealized positions [$d(C-H) = 0.96$ Å, $U = 1.2U_{iso}$ for the carbon to which it is attached]. The methyl groups were defined as rigid bodies and refined using group thermal parameters. The phenyl groups were refined as rigid, planar hexagons [$d(C-C) = 1.395$ Å], and the C_5 ring of the Cp^* ligand was refined as a rigid, planar pentagon [$d(C-C) = 1.420$ Å].

For $Cp^*(PMe_3)_2RuSi[S(Tol-p)](OTf)_2$ (7). Preliminary photographic characterization showed *mmm* Laue symmetry. Systematic absences uniquely defined the space group as $P2_12_1$. Refinement of a multiplicative term [1.05(18)] for Δ_f'' indicates that the chosen enantiomer is correct. An absorption correction was not applied (low μ , well-shaped crystal, $T_{max}/T_{min} = 1.014$). A Patterson synthesis located the Ru atom, and the remaining non-hydrogen atoms were located through subsequent least-squares and difference Fourier synthesis. All non-hydrogen and non-carbon atoms were included as idealized isotropic contributions [$d(C-H) = 0.96$ Å, $U = 1.2U_{iso}$ for the carbon to which it is attached].

For $\{Cp^*(PMe_3)_2RuSi[S(Tol-p)]_2(NCMe)\}BPh_4$ (13). Preliminary photographic characterization showed *mmm* Laue symmetry, and systematic absences in the diffraction data established the space group as $Pnma$ or $Pn2_1a$ (non-standard $Pna2_1$). E-statistics suggested the non-centrosymmetric alternative and the chemically sensible results of refinement showed that $Pn2_1a$ was the correct space group. Refinement of a multiplicative term [1.08 (12)] for Δ_f'' indicates that the enantiomer reported is correct. An absorption correction was not applied (low μ , well shaped crystals, $T_{max}/T_{min} = 1.012$). All non-hydrogen atoms, except those of the BPh_4^- anion, were refined with anisotropic thermal parameters. All hydrogen

atoms were included as idealized isotropic contributions [$d(\text{C—H}) = 0.96 \text{ \AA}$, $U = 1.2U_{\text{iso}}$ for the carbon to which it is attached] and the phenyl rings were constrained as rigid planar hexagons [$d(\text{C—C}) = 1.396 \text{ \AA}$].

For $[\text{Cp}^*(\text{PMe}_3)_2\text{RuSiMe}_2(\text{NCMe})]\text{BPh}_4$ (**15**). Photographic evidence indicated $2/m$ Laue symmetry and the space group was uniquely assigned from the observed systematic absences. No correction for absorption was required. The three legs of the piano-stool structure are rotationally disordered over two sites in a 78 : 22 ratio. The methyl groups are shared between sites and were refined at unit occupancy. The minority-site molecule of NCMe was not located. All non-hydrogen atoms were anisotropically refined, and hydrogen atoms were treated as idealized contributions [$d(\text{C—H}) = 0.96 \text{ \AA}$, $U = 1.2U_{\text{iso}}$ for the carbon to which it is attached].

Acknowledgment—We thank the National Science Foundation for support of this work.

REFERENCES

1. D. A. Straus, T. D. Tilley, A. L. Rheingold and S. J. Geib, *J. Am. Chem. Soc.* 1987, **109**, 5872.
2. C. Zybilla and G. Müller, *Angew. Chem., Int. Ed. Engl.* 1987, **26**, 669.
3. Observation of the unstable, amine-complexed $(\text{CO})_4\text{FeSiMe}_2(\text{NHEt}_2)$ had been reported previously: G. Schmid and E. Welz, *Angew. Chem., Int. Ed. Engl.* 1977, **16**, 785.
4. (a) T. D. Tilley, in *The Chemistry of Organic Silicon Compounds* (Edited by S. Patai and Z. Rappoport), Chapter 24, p. 1415. Wiley, New York (1989); (b) T. D. Tilley, in *The Silicon-Heteroatom Bond* (Edited by S. Patai and Z. Rappoport), Chapters 9 and 10, pp. 245 and 309. Wiley, New York (1991); (c) C. Zybilla, *Top. Curr. Chem.* 1991, **160**, 1; (d) C. Zybilla, *Adv. Organomet. Chem.* 1994, **36**, 229; (e) P. D. Lickiss, *Chem. Soc. Rev.* 1992, 271.
5. (a) C. Zybilla, D. L. Wilkinson and G. Müller, *Angew. Chem., Int. Ed. Engl.* 1988, **27**, 583; (b) C. Zybilla and G. Müller, *Organometallics* 1988, **7**, 1368; (c) C. Zybilla, D. L. Wilkinson, C. Leis and G. Müller, *Angew. Chem., Int. Ed. Engl.* 1989, **28**, 203; (d) C. Leis, C. Zybilla, J. Lachmann and G. Müller, *Polyhedron* 1991, **11**, 1163; (e) R. Probst, C. Leis, S. Gamper, E. Herdtweck and C. Zybilla, *Angew. Chem., Int. Ed. Engl.* 1991, **30**, 1132; (f) C. Leis, D. L. Wilkinson, H. Handwerker, C. Zybilla and G. Müller, *Organometallics* 1992, **11**, 514; (g) H. Handwerker, C. Leis, S. Gamper and C. Zybilla, *Inorg. Chim. Acta* 1992, **200**, 763; (h) H. Handwerker, C. Leis, R. Probst, P. Bissinger, A. Grohmann, P. Kiprof, E. Herdtweck, J. Blümel, N. Auner and C. Zybilla, *Organometallics* 1993, **12**, 2162; (i) H. Handwerker, M. Paul, J. Blümel and C. Zybilla, *Angew. Chem., Int. Ed. Engl.* 1993, **32**, 1313; (j) H. Handwerker, M. Paul, J. Riede and C. Zybilla, *J. Organomet. Chem.* 1993, **459**, 151.
6. (a) D. A. Straus, C. Zhang, G. E. Quimbata, S. D. Grumbine, R. H. Heyn, T. D. Tilley, A. L. Rheingold and S. J. Geib, *J. Am. Chem. Soc.* 1990, **112**, 2673; (b) S. D. Grumbine, R. K. Chadha and T. D. Tilley, *J. Am. Chem. Soc.* 1992, **114**, 1518; (c) C. Zhang, S. D. Grumbine and T. D. Tilley, *Polyhedron* 1991, **10**, 1173.
7. (a) K. Ueno, H. Tobita, M. Shimoi and H. Ogino, *J. Am. Chem. Soc.* 1988, **110**, 4092; (b) H. Tobita, K. Ueno, M. Shimoi and H. Ogino, *J. Am. Chem. Soc.* 1990, **112**, 3415; (c) T. Takeuchi, H. Tobita and H. Ogino, *Organometallics* 1991, **10**, 835; (d) J. Koe, H. Tobita and H. Ogino, *Organometallics* 1992, **11**, 2479; (e) K. Ueno, H. Tobita and H. Ogino, *J. Organomet. Chem.* 1992, **430**, 93; (f) K. Ueno, H. Tobita, S. Seki and H. Ogino, *Chem. Lett.* 1993, 1723.
8. (a) R. Corriu, G. F. Lanneau and C. Priou, *Angew. Chem., Int. Ed. Engl.* 1991, **9**, 1130; (b) R. J. Corriu, G. F. Lanneau and P. S. Chauhan, *Organometallics* 1993, **12**, 2001.
9. P. Jutzi and A. Möhrke, *Angew. Chem., Int. Ed. Engl.* 1990, **29**, 893.
10. L. K. Woo, D. A. Smith and V. G. Young Jr, *Organometallics* 1991, **10**, 3977.
11. K. E. Lee, A. M. Arif and J. A. Gladysz, *Chem. Ber.* 1991, **124**, 309.
12. N. Wiberg, K. Schurz, G. Reber and G. Müller, *J. Chem. Soc., Chem. Commun.* 1986, 591.
13. (a) N. Wiberg, G. Wagner, G. Reber, J. Riede and G. Müller, *Organometallics* 1987, **6**, 35; (b) N. Wiberg and G. Wagner, *Chem. Ber.* 1986, **119**, 1467.
14. (a) Z. Xie, D. J. Liston, T. Jelínek, V. Miřro, R. Bau and C. A. Reed, *J. Chem. Soc., Chem. Commun.* 1993, 384; (b) A. R. Bassindale and T. Stout, *Tetrahedron Lett.* 1985, **26**, 3403; (c) K. Hensen, T. Zengerly, P. Pickel and G. Klebe, *Angew. Chem., Int. Ed. Engl.* 1983, **22**, 725; (d) J. B. Lambert, S. Zhang, C. L. Stern and J. C. Huffman, *Science* 1993, **260**, 1917; (e) G. K. S. Prakash, S. Keyaniyan, R. Aniszfeld, L. Heiliger, G. A. Olah, R. C. Stevens, H.-K. Choi and R. Bau, *J. Am. Chem. Soc.* 1987, **109**, 5123; (f) G. A. Olah, L. Heiliger, X.-Y. Li and G. K. S. Prakash, *J. Am. Chem. Soc.* 1990, **112**, 5991; (g) C. A. Reed, Z. Xie, R. Bau and A. Benesi, *Science* 1993, **262**, 402; (h) R. J. P. Corriu and M. Henner, *J. Organomet. Chem.* 1974, **74**, 1.
15. (a) R. L. School, G. E. Maciel and W. K. Musker, *J. Am. Chem. Soc.* 1972, **94**, 6376; (b) E. A. Williams, *Annu. Reports NMR Spectrosc.* 1983, **15**, 235.
16. D. A. Straus, S. D. Grumbine and T. D. Tilley, *J. Am. Chem. Soc.* 1990, **112**, 7801.
17. S. K. Grumbine, T. D. Tilley, F. P. Arnold and A. L. Rheingold, *J. Am. Chem. Soc.* 1994, **116**, 5495.
18. S. D. Grumbine, T. D. Tilley, F. P. Arnold and A. L. Rheingold, *J. Am. Chem. Soc.* 1993, **115**, 7884.
19. S. D. Grumbine, T. D. Tilley and A. L. Rheingold, *J. Am. Chem. Soc.* 1993, **115**, 358.

20. M. Denk, R. K. Hayashi and R. West, *J. Chem. Soc., Chem. Commun.* 1994, 33.
21. G. A. Lawrance, *Chem. Rev.* 1986, **86**, 17.
22. W. J. Geary, *Coord. Chem. Rev.* 1971, **7**, 81.
23. S. K. Grumbine, Ph.D. Thesis, University of California, San Diego, California (1993).
24. W. Adam, U. Azzena, F. Prechtel, K. Hindahl and W. Malisch, *Chem. Ber.* 1992, **125**, 1409.
25. N. Wiberg, G. Wagner, G. Müller and J. Riede, *J. Organomet. Chem.* 1984, **271**, 381.
26. D. L. Lichtenberger and A. Rai-Chaudhuri, *J. Am. Chem. Soc.* 1991, **113**, 2923.
27. W. Petz, *Chem. Rev.* 1986, **86**, 1019.
28. H. Bock, M. Kremer, M. Dolg and H.-W. Preuß, *Angew. Chem., Int. Ed. Engl.* 1991, **30**, 1186.
29. (a) A. Haaland, *Angew. Chem., Int. Ed. Engl.* 1989, **28**, 992; (b) G. Klebe, K. Hensen and H. Fuess, *Chem. Ber.* 1984, **117**, 797; (c) G. Klebe, *Chem. Ber.* 1985, **293**, 147.
30. (a) M. T. Rogers and J. C. Woodbrey, *J. Phys. Chem.* 1962, **66**, 540; (b) J. Sandström, *Dynamic NMR Spectroscopy*. Academic Press, New York (1982).
31. P. P. Gaspar, D. Holten, S. Konieczny and J. Y. Corey, *Acc. Chem. Res.* 1987, **20**, 329, and references cited therein.
32. M. Ishikawa and M. Kumada, *Adv. Organomet. Chem.* 1981, **19**, 51.
33. (a) K. L. Jones and K. H. Pannell, *J. Am. Chem. Soc.* 1993, **115**, 11336; (b) K. H. Pannell, M.-C. Brun, H. Sharma, K. Jones and S. Sharma, *Organometallics* 1994, **13**, 1075; (c) K. H. Pannell, J. Cervantes, C. Hernandez, J. Cassias and S. Vincenti, *Organometallics* 1986, **5**, 1056; (d) K. H. Pannell, J. M. Rozell Jr and C. Hernandez, *J. Am. Chem. Soc.* 1989, **111**, 4482; (e) K. H. Pannell, L.-J. Wang and J. M. Rozell, *Organometallics* 1989, **8**, 550; (f) H. Tobita, K. Ueno and H. Ogino, *Bull. Chem. Soc. Jpn.* 1988, **61**, 2797; (g) K. Ueno, H. Tobita and H. Ogino, *Chem. Lett.* 1990, 369; (h) A. Haynes, M. W. George, M. T. Haward, M. Poliakoff, J. J. Turner, N. M. Boag and M. Green, *J. Am. Chem. Soc.* 1991, **113**, 2011.
34. Y. Apeloig, S. A. Godleski, D. J. Heacock and J. M. McKelvey, *Tetrahedron Lett.* 1981, 3297.
35. T. D. Tilley, R. H. Grubbs and J. E. Bercaw, *Organometallics* 1984, **3**, 274.
36. L. Birkofer and O. Stuhl, in *The Chemistry of Organic Silicon Compounds* (Edited by S. Patai and Z. Rapoport), Chapter 10, p. 655. Wiley, New York (1989).